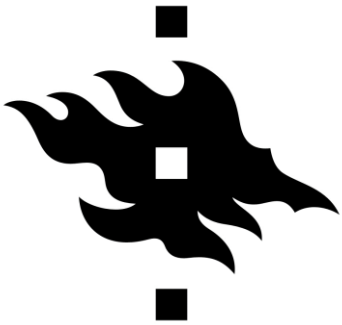

HELSINGIN YLIOPISTO
HELSINGFORS UNIVERSITET
UNIVERSITY OF HELSINKI

Calsyntenin-3 Laminin G-Like Domain Forms Dimers in a Solution

Taru Larkiala

11/2020

Master's Thesis

Faculty of Biological and Environmental Sciences

Master's Programme in Genetics and Molecular Biosciences

HELSINGIN YLIOPISTO
HELSINGFORS UNIVERSITET
UNIVERSITY OF HELSINKI

Faculty	Degree Programme
Faculty of Biological and Environmental Sciences	Master's Programme in Genetics and Molecular Biosciences

Author

Taru Katariina Larkiala

Title

Calsyntenin-3 Laminin G-Like Domain Forms Dimers in a Solution

Subject/Study track

Biochemistry and Structural Biology

Level	Month and year	Number of pages
Master's Thesis	11/2020	48 + 4 appendices

Abstract

Calsyntenin-3 is a type I transmembrane protein, that is mainly expressed on the post-synaptic cell membranes. It belongs to the calsyntenin family that is part of the cadherin superfamily. Calsyntenin-3 consists of a cytosolic C-terminal region, a transmembrane domain and an extracellular N-terminal part, that consists of a laminin G-like domain (LNS) and two cadherin domains (CAD). Calsyntenin-3 is mainly expressed in the brain, but it can also be found in the heart, liver, pancreas, lung, skeletal muscle and placenta. Calsyntenin-3 has an effect on neurogenesis by affecting the development of excitatory and inhibitory synapses. It might also play a role in Alzheimer's disease, as it has been found to be able to bind β-amyloid peptide, that is known to play a key role in the development of Alzheimer's disease.

Calsyntenin-3 acts as a synaptic adhesion protein, that binds to the post-synaptic neurexins with its extracellular region. However, the previous studies have contradicting results regarding the calsyntenin-3 domains that mediate the interaction between the calsyntenin-3 and neurexins. There is also disagreement whether calsyntenin-3 binds neurexin-α, neurexin-β or both. Because of these discrepancies, the aim of this master's thesis study was to produce the calsyntenin-3 ectodomain constructs that contained either the two CAD domains, the LNS domain or all three domains, using baculovirus mediated protein production in insect cell cultures. These purified protein constructs were meant to be used for the determination of the binding domains. Unfortunately, only the purification of the calsyntenin-3 LNS domain was successful and the purification of the constructs, containing the CAD domains, was unsuccessful. A SEC-MALLS experiment, that was performed for the calsyntenin-3 LNS domain, revealed that it forms dimers in a solution, which is consistent with experiments performed with the LNS domain of human sex hormone-binding globulin.

The second aim of this master's thesis study was to express the calsyntenin-3 ectodomain constructs on the surface of HEK293T cells and to test the binding between calsyntenin-3 and neurexins in a cell surface binding assay. The results of the cell surface binding assay indicated that the binding is mediated by the calsyntenin-3 CAD domains and that calsyntenin-3 binds to neurexin-α, but the binding to neurexin-β was not detected. However, the results from the cell surface binding assay were conflicting: the binding between the calsyntenin-3 full ectodomain construct and neurexin-α was not detected, but the binding was detected between calsyntenin-3 CAD ectodomain construct and neurexin-α. Therefore, the cell surface binding assay cannot be considered entirely reliable and should be repeated before making further conclusions.

Keywords

Calsyntenin-3, Neurexin, LNS domain, CAD domain, Recombinant baculovirus protein production, Sf9 cells, High Five cells, Cell surface binding assay

Supervisors

Tommi Kajander, Ph.D., and Sudeep Karki M.Sc.

Where deposited

E-Thesis, University of Helsinki

HELSINGIN YLIOPISTO
HELSINGFORS UNIVERSITET
UNIVERSITY OF HELSINKI

Tiedekunta	Koulutusohjelma
Bio- ja ympäristötieteellinen tiedekunta	Genetiikan ja molekulaaristen biotieteiden maisteriohjelma

Tekijä

Taru Katariina Larkiala

Työn nimi

Kalsynteniini-3:n laminiinin G-domeenin tyyppinen -domeeni muodostaa dimeerejä liuoksessa

Oppiaine/Opintosuunta

Biokemia ja rakennebiologia

Työn laji	Aika	Sivumäärä
Pro gradu -tutkielma	11/2020	48 + 4 liitettä

Tiivistelmä

Kalsynteniini-3 on tyypin I kalvoproteiini, jota esiintyy pääasiassa post-synaptisissa solukalvoissa. Se kuuluu kalsynteniinien proteiiniperheeseen, joka on osa kadheriinien superperhettä. Kalsynteniini-3 sisältää solulimanpuoleisen C-terminaalisen osan, kalvon läpäisevän domeenin ja solunulkoisen N-terminaalisen osan, joka sisältää laminiinin G-domeenin tyyppisen -domeenin (LNS) ja kaksi kadheriinidomeenia (CAD). Kalsynteniini-3:a esiintyy pääasiassa aivoissa, mutta sitä on myös sydämessä, maksassa, haimassa, keuhkoissa, lihaksissa ja istukassa. Kalsynteniini-3:lla on vaikutusta neurogeneesiin, sillä se vaikuttaa eksitatoristen ja inhibitoristen synapsien kehitykseen. Sillä voi olla myös vaikutusta Alzheimerin taudin kehittymisessä, koska sen on havaittu pystyvän sitoutumaan β-amyloidipeptidiin, jonka tiedetään olevan avainasemassa Alzheimerin taudin synnyssä.

Kalsynteniini-3 on synaptinen adheesioproteiini, joka sitoutuu postsynaptisiin neureksiineihin solunulkoisella osallaan. Aikaisempien tutkimusten tulokset ovat kuitenkin ristiriidassa keskenään sen suhteen, mikä kalsynteniini-3:n domeeni sitoutuu neureksiineihin. Erimielisyyttä esiintyy myös siitä, sitoutuuko kalsynteniini-3 neureksiini-α:aan, neureksiini-β:aan vai molempiin. Näiden ristiriitojen takia tämän pro gradu -työn tavoitteena oli tuottaa rekombinanttien bakulovirusten avulla hyönteissoluviljelmissä osia kalsynteniini-3:sta siten, että ne sisälsivät joko kalsynteniini-3:n kaksi CAD-domeenia, LNS-domeenin tai kaikki kolme domeenia. Nämä puhdistetut kalsynteniini-3:n osat olisi käytetty kokeissa, joissa olisi määritelty, mitkä kalsynteniini-3:n domeenit sitoutuvat neureksiineihin. Valitettavasti vain kalsynteniini-3:n LNS-domeenin puhdistus onnistui ja CAD-domeeneja sisältävien rakenteiden puhdistus epäonnistui. SEC-MALLS-koe, joka tehtiin kalsynteniini-3:n LNS-domeenille, paljasti, että kalsynteniini-3:n LNS-domeeni muodostaa dimeerejä liuoksessa, mikä on yhdenmukaista sukupuolihormoneja sitovan globuliinin LNS-domeenilla tehtyjen kokeiden kanssa.

Tämän pro gradu -työn toinen tavoite oli ilmentää kalsynteniini-3:n osia HEK293T-solujen pinnalla, ja testata kalsynteniini-3:n ja neureksiinien sitoutumista solun pinnalla tehtävässä sitoutumiskokeessa. Sitoutumiskokeen tulokset viittaavat siihen, että sitoutuminen tapahtuu kalsynteniini-3:n CAD-domeenien avulla, ja että kalsynteniini-3 sitoutuu neureksiini-α:aan, mutta ei neureksiini-β:aan. Sitoutumiskokeen tulokset olivat kuitenkin ristiriitaisia: sitoutumista kalsynteniini-3:n täyspitkän solunulkoisen osan ja neureksiini-α:n välillä ei havaittu, mutta sitoutumista havaittiin pelkän kalsynteniini-3:n CAD-domeenin sisältävän proteiinin ja neureksiini-α:n välillä. Tämän vuoksi solun pinnan sitoutumismääritystä ei voida pitää täysin luotettavana, ja se tulisi toistaa ennen uusien johtopäätösten tekemistä.

Avainsanat

Kalsynteniini-3, Neureksiini, LNS-domeeni, CAD-domeeni, Rekombinantti bakuloviruksen proteiinituotanto, Sf9-solut, High Five -solut, Sitoutumistesti solun pinnalla

Ohjaajat

Tommi Kajander, FT, ja Sudeep Karki, M.Sc.

Säilytyspaikka

E-Thesis, Helsingin yliopisto

TABLE OF CONTENTS

ABBREVIATIONS

Aβ	β-amyloid peptide
APP	β-amyloid protein precursor
CAD	Cadherin domain
CLSTN	Calsyntenin
CLSTN1	Calsyntenin-1
CLSTN2	Calsyntenin-2
CLSTN3	Calsyntenin-3
CTF	C-terminal fragment
DMEM	Dulbecco's Modified Eagle's medium
DMEM+FBS	0.5% FBS supplemented DMEM pH 7.4 media
EGF	Epidermal growth factor-like domain
FBS	Fetal bovine serum
Fc	Human IgG1 Fc
GST	Glutathione-s-transferase
HEK293T	Human embryonic kidney 293T cell line
High Five	BTI-TN-5B1-4 *Trichoplusia ni* cell line
KLC1	Kinesin-1 light chain-1
LB	Lysogeny broth
LNS	Laminin G-like domain also called Laminin, Neurexin, Sex hormone-binding globulin
NRXN	Neurexin
NTF	N-terminal fragment
PBS	Phosphate-buffered saline
PEI	Polyethyleneimine
PFA	Paraformaldehyde
PSP	PreScission Protease
PVDF	Polyvinylidene fluoride
SEC	Size-exclusion chromatography
SEC-MALLS	The size-exclusion chromatography-coupled multi-angle static laser light scattering
SFX medium	HyClone SFX-Insect insect cell culture medium
SOC	Super Optimal Broth
SS4	Splice site 4
TBS	Tris-buffered saline
TBS-T	TBS buffer containing 0.5% TWEEN® 20
X11L	X11-like protein

1. BACKGROUND

1.1 CALSYNTENINS

Calsyntenins (CLSTNs) are a family of transmembrane proteins expressed mainly in the brain (Hintsch et al., 2002; Vogt et al., 2001). The CLSTN family belongs to the cadherin superfamily and consists of three members that are called calsyntenin-1, -2 and -3. They are all type I transmembrane proteins that have a cytosolic C-terminal region, a transmembrane domain and an extracellular N-terminal part that consists of a laminin G-like domain (LNS) and two cadherin domains (CAD) (Hintsch et al., 2002; Vogt et al., 2001). Calsyntenin-1 (CLSTN1) was first found in embryonic spinal cord neurons in chickens and named calsyntenin because of its ability to bind calcium with its cytosolic domain (Vogt et al., 2001). In a follow-up study calsyntenin-2 (CLSTN2) and calsyntenin-3 (CLSTN3) were also discovered, but interestingly they were found not to be able to bind calcium (Hintsch et al., 2002).

CLSTNs were also independently discovered by another group, while they were looking for proteins that associate with X11-like protein (X11L) (Araki et al., 2003). X11L binds and can inhibit the proteolytical processing of β-amyloid protein precursor (APP) that is essential in the development of Alzheimer's disease. Another family of proteins, alcadeins (Alzheimer's disease-related cadherin-like proteins) were found to form a complex with X11L. From this new family of proteins alcadein-α and alcadein-β were associating with the X11L and the X11L/APP complex. Alcadein-α, alcadein-β and alcadein-γ correlates with CLSTN1, CLSTN3 and CLSTN2, respectively (Araki et al., 2003). In this thesis, these proteins will be referred to as calsyntenins.

The calsyntenin genes are conserved throughout the animal kingdom from *Caenorhabditis elegans* and *Drosophila melanogaster* to humans (Vogt et al., 2001). Mammals, fish and birds all have three calsyntenin genes but *C. elegans* and *D. melanogaster* only have one calsyntenin gene, which are named casy-1 and Cals, respectively (Vogt et al., 2001). Human calsyntenin genes share a sequence identity of ~50% with each other (Hintsch et al., 2002; Vogt et al., 2001). Human calsyntenin genes have a sequence identity of over 90% overall in mammals, ~80% with the equivalent chicken calsyntenin genes and 60% – 75% with the equivalent zebrafish calsyntenin genes. Human

calsyntenin-1 and calsyntenin-2 genes have ~30% sequence identity with the *D. melanogaster* Cals gene and *C. elegans* casy-1 gene, respectively. The sequence alignments and the identity matrices of human, mouse, chicken, zebrafish, *D. melanogaster* and *C. elegans* calsyntenin genes are shown in Appendix 1.

The CLSTNs have different expression patterns in the human tissues. All of the three CLSTNs are mainly expressed in the brain, but CLSTN1 and CLSTN3 are also expressed in other tissues in humans (Hintsch et al., 2002; Vogt et al., 2001). In addition to the expression in the brain, CLSTN1 is also found in the kidney, skeletal muscle, heart and placenta (Hintsch et al., 2002; Vogt et al., 2001). CLSTN3 has most expression in the brain and the kidney, but it can also be found in the heart, liver, pancreas, lung, skeletal muscle and placenta in humans (Hintsch et al., 2002; Vogt et al., 2001).

1.1.1 CALSYNTENINS MAY PLAY A ROLE IN ALZHEIMER'S DISEASE

Alzheimer's disease is a neurodegenerative disease that causes dementia and eventually leads to death. In Alzheimer's disease, amyloid fibrils, that consist of the pathogenic β-amyloid peptide (Aβ), have accumulated in the brain (Glenner and Wong, 1984; Jarrett et al., 1993). Normally, APP is proteolytically processed by α-secretase at the α-site which leads to a formation of two fragments, a C-terminal fragment-α (CTF-α) and an extracellular N-terminal fragment-α (NTF-α), that are non-pathogenic (Esch et al., 1990). The APP CTF-α is further processed by γ-secretase and forms the p3 peptide and the intracellular fragment (Haass et al., 1993). In Alzheimer's disease, APP is cleaved by β-secretase that cleaves APP at the β-site. This leads to a formation of a C-terminal fragment-β (CTF-β) and an extracellular N-terminal fragment-β (NTF-β). The APP CTF-β is further processed by γ-secretase, producing the pathogenic Aβ (Seubert et al., 1993). The proteolytical cleavage of APP can be inhibited by binding of X11L, that can form a complex with APP or the APP CTF-α and -β. The complex prevents the proteolytical processing by γ-secretase. Also, CLSTN1 and CLSTN3 can regulate the APP cleavage by binding APP or the APP CTF-β through a tripartite complex that involves also X11L (Araki et al., 2003).

CLSTN1, CLSTN2 and CLSTN3 are proteolytically processed in a similar manner as APP (Araki et al., 2004; Hata et al., 2009). CLSTNs are first cleaved by α-secretase, forming an NTF-α and a CTF-α. The α-secretase cleavage site in CLSTNs is located near the transmembrane region at the extracellular part of the protein. After that, the CTF-α is cleaved by γ-secretase, forming an intracellular domain and a secreted p3-like peptide. The γ-secretase cleavage site is located between the α-secretase cleavage site and the transmembrane region in CLSTNs (Hata et al., 2009). The domain structures and the proteolytical processing of CLSTNs are presented in the Figure 1.1.

The dysfunction of γ-secretase, that is related to some sporadic cases of Alzheimer's disease, also affect the proteolytical processing of CLSTNs (Hata et al., 2009). Therefore, it has been suggested that the CLSTNs could be used as biomarkers for Alzheimer's disease in the pre-pathogenic phase in some cases (Hata et al., 2009). CLSTNs can be isolated from the human cerebrospinal fluid, and the changes in the proteolytical processing of the CLSTNs could be measured. If changes are detected, it could mean dysfunction of γ-secretase, that could lead to Alzheimer's disease (Hata et al., 2009).

The CLSTNs bind to kinesin-1 light chain-1 (KLC1) with their KCL1-binding segments (KBS), which are located in their C-terminal domain. Kinesin-1 acts as a motor protein, that for example in neuronal cells delivers vesicle cargo from the *trans*-Golgi network to the axonal periphery (Konecna et al., 2006). In CLSTN1 and CLSTN2 there are two KBS in the C-terminus but in CLSTN3 there is only one KBS, as shown in Figure 1.1. Therefore, CLSTN1 and CLSTN2 bind KLC1 more strongly than CLSTN3. Even though all of the CLSTNs have the ability to bind KLC1, CLSTN3 was not found to be able to act as a cargo docking protein (Konecna et al., 2006).

Both, APP and CLSTN1 are located at the *trans*-Golgi network, where they are mostly co-localized but can also occur independently (Araki et al., 2007; Ludwig et al., 2009). The co-localization of CLSTN1 and APP might be mediated by X11L (Araki et al., 2003). CLSTN1 and APP form a complex that prevents the proteolytical processing of APP (Steuble et al., 2012). APP and CLSTN1 are transported from the *trans*-Golgi network to the axonal periphery. Kinesin-1 motor protein transports both CLSTN1- and APP-containing secretory vesicles along the axons. CLSTN1 and APP can be transported in separate vesicles or co-transported in the same vesicle (Araki et al., 2007; Ludwig et al., 2009; Steuble et al., 2010; Steuble et al., 2012). However, preventing CLSTN1 from exiting the *trans*-Golgi network, inhibited also the APP from exiting the *trans*-Golgi network, implying that APP transport is CLSTN1 dependent (Ludwig et al., 2009).

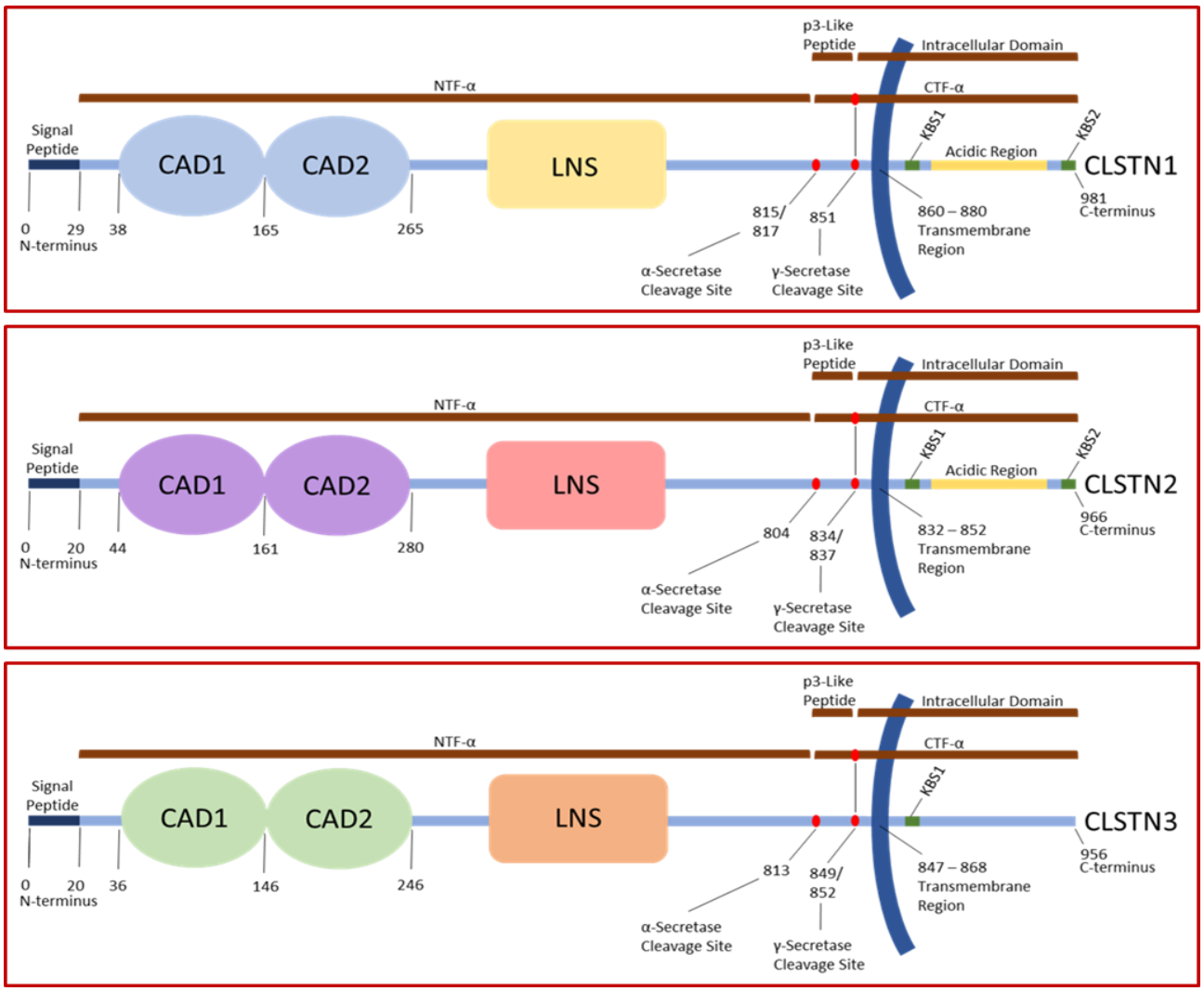

Figure 1.1 Domain Structure and Proteolytical Processing of Human CLSTNs

All three CLSTNs have a signal peptide, two CAD-domains and an LNS-domain, that are located at the extracellular N-terminal region. The α- and γ-secretase cleavage sites are at the extracellular region, near the transmembrane region. The proteolytical processing of CLSTNs by α-secretase leads to NTF-α and CTF-α. Further processing of CTF-α by γ-secretase leads to formation of the p3-like peptide and the intracellular domain. All CLSTNs have kinesin-1 light chain-1 binding sites (KBS) in their intracellular region. CLSTN1 and CLSTN2 have two KBS, while CLSTN3 has only one KBS. Because CLSTN3 has only one KBS, its binding to kinesin-1 is weaker than that of CLSTN1 and CLSTN2.

Kinesin-1 transports both the CLSTN1/APP- and only CLSTN1-containing vesicles to the axonal periphery, where they fuse with the sorting endosome and the plasma membrane, respectively. β-secretase can be transported within the same vesicles as CLSTN1 and APP. CLSTN1 protects APP from being proteolytically cleaved during the vesicle transport to the axonal periphery (Steuble et al., 2012). The CLSTN1/APP-containing vesicle fuses to the sorting endosome at the axonal periphery. The full-length CLSTN1 is recycled to the slow recycling endosomes and the full-length APP can be proteolytically cleaved by β- and γ-secretases at the endosome or recycled to the plasma

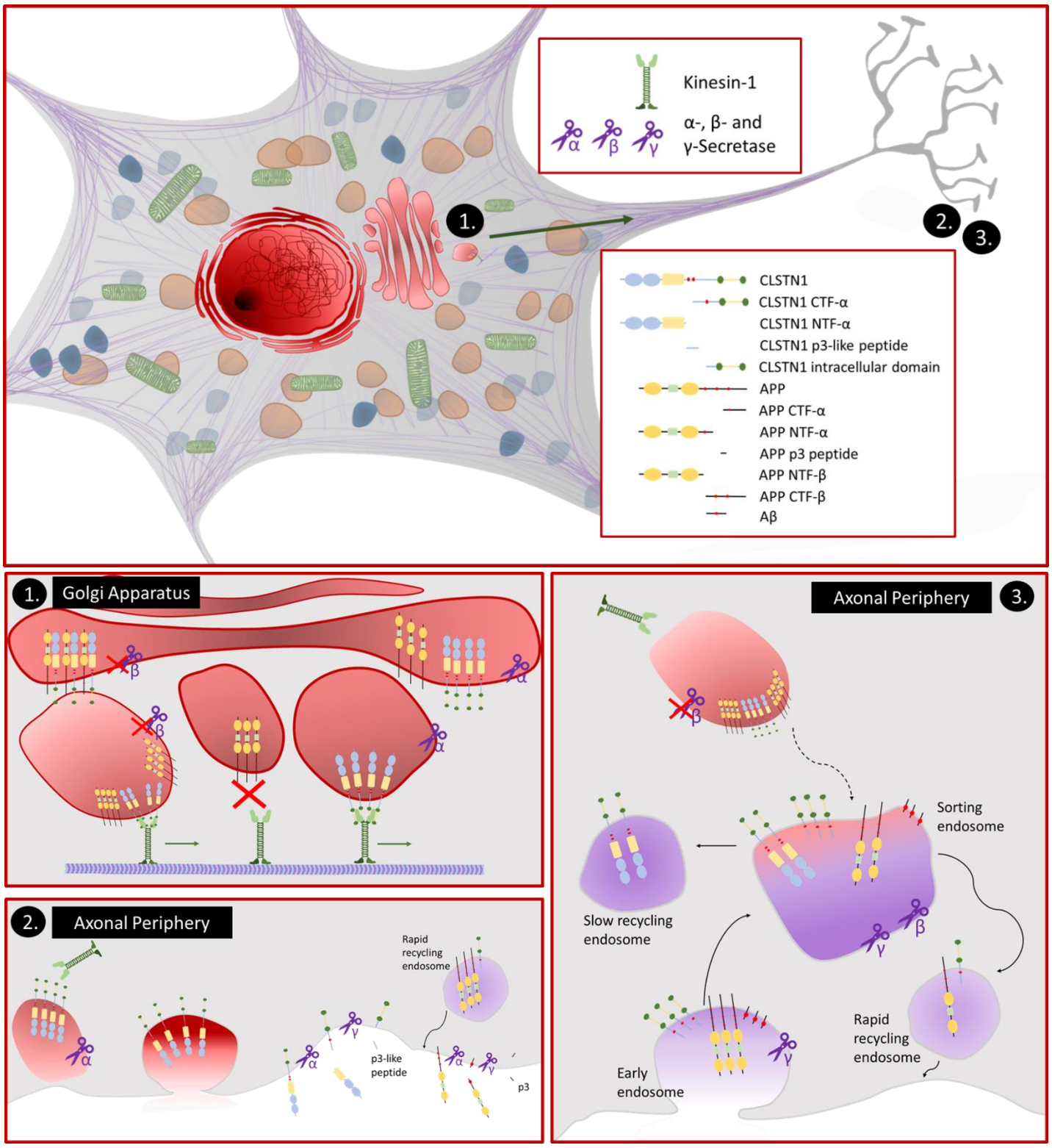

Figure 1.2 CLSTN1 and APP Trafficking and Proteolytical Processing in the Neuronal Cell

1.) CLSTN1 and APP are co-localized at the *trans*-Golgi network. CLSTN1 connects the APP-containing vesicle to the motor protein kinesin-1, that transports the vesicle to the axonal periphery. The vesicle containing only APP and not CLSTN1, cannot bind to kinesin-1. CLSTN1 forms a complex with APP, preventing the proteolytical cleavage of APP by β-secretase during the transport. The transported vesicle is fused to the early endosome (3.). CLSTN1 can be transported also independently. Kinesin-1 transports the vesicle to the axonal periphery where the vesicle is fused to the plasma membrane (2.). CLSTN1 might be at least partly cleaved by α-secretase already during the transportation. **2.)** After the transported CLSTN1-containing vesicle has been fused to the cell

membrane, α-secretase can cleave CLSTN1, forming the CLSTN1 CTF-α and the secreted CLSTN1 NTF-α. After that, the γ-secretase cleaves CLSTN1 CTF-α, forming the p3-like peptide and the intracellular domain. APP is also proteolytically processed at the plasma membrane. APP arrives to the plasma membrane in a rapid recycling endosome, that is fused to the plasma membrane. After that, α-secretase can cleave APP, forming the APP CTF-α and the secreted APP NTF-α. Then, the γ-secretase cleaves APP CTF-α, forming the p3 peptide and the intracellular fragment. **3.)** The full-length CLSTN1/APP-containing vesicle arrives to the axonal periphery and fuses to the sorting endosome. The sorting endosome separates the full-length CLSTN1 and recycles it to the slow recycling endosomes. Early endosomes, that contain cleaved CLSTN1, and both cleaved and full-length APP, are arriving from the plasma membrane and fuse to the sorting endosome. The uncleaved APP can be proteolytically processed by β-secretase at the endosome, forming the APP NTF-β and CTF-β, that can then be cleaved by γ-secretase, forming the Aβ peptide. The full-length APP can also be recycled to the plasma membrane in rapid recycling endosomes.

membrane in a rapid recycling endosome (Steuble et al., 2010). The full-length APP can be cleaved at the plasma membrane by α- and γ-secretases. APP is re-endocytosed from the plasma membrane partly in the full-length form and partly in the cleaved form (Steuble et al., 2010). The vesicle containing only CLSTN1 includes α-secretase, that can cleave CLSTN1 already during the transportation to the plasma membrane (Maruta et al., 2012). The remaining full-length CLSTN1 is cleaved at the plasma membrane and the intracellular domain is moved to an early endosome by endocytosis (Steuble et al., 2010). The CLSTN1 and APP trafficking and proteolytical processing is presented in the Figure 1.2. The proteolytical processing and the trafficking of CLSTNs and APP are connected to each other, which suggests that CLSTNs may also be linked to Alzheimer's disease.

1.1.2 CALSYNTENIN-2 HAS AN EFFECT ON MEMORY AND LEARNING

In a genome-wide screening study, a T/C single nucleotide polymorphism in the first intron of the CLSTN2 gene was found to be associated to human episodic memory performance (Papassotiropoulos et al., 2006). Together, a frequent T → C substitution in the CLSTN2 gene and a C → T substitution in the KIBRA (kidney and brain expressed protein) gene, was shown to affect beneficially for the human episodic memory performance (Papassotiropoulos et al., 2006; Preuschhof et al., 2010). The CLSTN2 C-allele was also shown to have a favourable effect on the verbal memory in subjects without the KIBRA C → T substitution (Jacobsen et al., 2009). Conversely, the CLSTN2 TT-genotype is associated to worse semantic memory in old-age subjects (Laukka et al., 2013) and especially old-age subjects with depression (Pantzar et al., 2014).

Studies, done using mice and *C. elegans,* have also shown that CLSTN2 and its ortholog CASY-1 in *C. elegans* have an effect on learning and memory (Hoerndli et al., 2009; Ikeda et al., 2008; Lipina et al., 2016). In mice, a deletion of CLSTN2 genes resulted in hyperactivity and poorer learning and memory performance, which was due to loss of parvalbumin-positive interneurons (Lipina et al., 2016). In *C. elegans*, loss of casy-1 results in impaired learning and memory performance (Ikeda et al., 2008). It was shown that only the LNS domain of CASY-1 was required to save the function in memory and learning, and the deletion of CAD domains, the intracellular and transmembrane regions seem to have no effect on the function (Ikeda et al., 2008). Interestingly, also the human CLSTN2 was able to save the impaired learning and memory in *C. elegans*, lacking the casy-1 gene (Hoerndli et al., 2009). It was also shown that, CASY-1 regulates the GABA release in neuromuscular junction by participating in the vesicle transport, and thus replacing also the function of CLSTN1 in *C. elegans* (Thapliyal et al., 2018).

1.1.3 CALSYNTENINS AFFECT SYNAPTOGENESIS

All CLSTNs have an effect on neuronal development. CLSTN1 affects excitatory synapse development, CLSTN2 inhibitory synapse development and CLSTN3 both excitatory and inhibitory synapse development (Lipina et al., 2016; Pettem et al., 2013; Ster et al., 2014). The regulation of axonal transport is necessary for the neuronal development and maturation. CLSTN1 was shown to affect neuronal development by regulating the axonal transportation of vesicles to the developing axons and by guiding specific endosomes to specific locations or axonal compartments (Alther et al., 2016; Ponomareva et al., 2014; Ster et al., 2014). CLSTN1 also regulates and organizes the microtubule highway in developing axons and thus regulates the cargo delivery to the developing axons (Lee et al., 2017).

CLSTN2 and CLSTN3 affect the synapse development by reducing the synapse transmission (Lipina et al., 2016; Pettem et al., 2013). Mice, lacking the Clstn2 genes, had a decreased number of parvalbumin-positive interneurons, which led to a decrease in inhibitory synapse transmission (Lipina et al., 2016). Like the deletion of Clstn2 genes, also the deletion of Clstn3 genes had a decreasing effect in synapse density (Kim et al., 2020; Pettem et al., 2013; Um et al., 2014). The full-

length CLSTN3 activates the differentiation of excitatory and inhibitory synapses by binding NRXN, but the cleaved ectodomain of CLSTN3 represses synaptic differentiation by blocking the NRXN-binding of other synaptogenic proteins, such as neuroligin-2 and LRRTM2 (Pettem et al., 2013).

Since the CLSTNs were discovered twenty years ago, the understanding of their function and role in the nervous system has started to take shape. Nevertheless, a lot remains to be discovered. CLSTNs are mainly expressed in the brain, where they have different but overlapping expression patterns and functions: CLSTN1 and CLSTN3, together with X11L, associate with APP and prevent its premature cleavage, CLSTN2 has a role in memory and learning, and CLSTN1, CLSTN2 and CLSTN3 all promote synapse differentiation and neuronal circuit formation (Araki et al., 2003; De Ramon Francàs et al., 2017; Lipina et al., 2016; Papassotiropoulos et al., 2006; Pettem et al., 2013; Ster et al., 2014). All CLSTNs occur in both cleaved and full-length form and it seems that the different forms have different functions: the cleaved and full-length forms of CLSTN1 are involved in vesicle transport of different types of vesicles and the cleaved and full-length forms of CLSTN3 seem to have an opposite effect in synapse differentiation (Araki et al., 2007; Ludwig et al., 2009; Pettem et al., 2013; Steuble et al., 2010; Steuble et al., 2012). The majority of studies about CLSTNs have focused on CLSTN1. Therefore, the roles of CLSTN2 and CLSTN3 are still largely unknown and more research needs to be conducted to get a better understanding of their functions.

1.2 NEUREXINS

Neurexins (NRXNs) are a family of type I transmembrane proteins that are present mostly on the surface of neurons (Ullrich et al., 1995; Ushkaryov et al., 1992; Ushkaryov et al., 1994). NRXNs are located on the presynaptic cell membranes of excitatory and inhibitory synapses at central and peripheral nervous system, where they affect synaptic transmission and act as synaptic adhesion molecules (Etherton et al., 2009; Ichtchenko et al., 1995; Kattenstroth et al., 2004; Kim et al., 2020; Lu et al., 2014; Missler et al., 2003; Pettem et al., 2013; Sons et al., 2006; Um et al., 2014; Ushkaryov et al., 1995; Zhang et al., 2010). Malfunction of NRXNs has been linked to schizophrenia and autistic spectrum disorder (Reichelt et al., 2012).

In humans, there are three genes coding for NRXNs: *NRXN1*, *NRXN2* and *NRXN3* (Ullrich et al., 1995; Ushkaryov et al., 1992; Ushkaryov et al., 1994). Each of these genes have two promoters, one of which codes for the longer NRXN-α and the other codes for the shorter NRXN-β. NRXN-α extracellular region consists of a signal peptide, six LNS domains, three epidermal growth factor-like (EGF) domains and there are also five alternative splice sites (SS1 – SS5) in the sequence coding for NRXN-α. NRXN-β is shorter than NRXN-α and its extracellular region consists of a signal peptide, NRXN-β specific histidine rich area and an LNS domain identical to the sixth LNS domain of NRXN-α. In the sequence, coding for NRXN-β, there are two alternative splice sites that are equal to the two last alternative splice sites of NRXN-α (SS4 and SS5) (Ullrich et al., 1995). It has been observed that NRXNs have different functions, although it is also known that NRXNs can replace each other in a rescue experiment (Dai et al., 2019; Zhang et al., 2005). The domain structures of NRXN-α and -β are presented in the Figure 1.3.

NRXNs have several postsynaptic ligands, such as CLSTN3, GABA-A receptors, leucine-rich repeat transmembrane proteins and neuroligins (Ichtchenko et al., 1995; Ko et al., 2009; Pettem et al., 2013; Zhang et al., 2010). NRXN ligand binding is dependent of the alternative splicing of NRXNs, especially of the SS4 insert, and the NRXN-α and -β variants. For example, leucine-rich repeat transmembrane proteins seem to be binding only NRXNs that do not include the insert at the SS4. However, neuroligins can bind NRXNs regardless of the insert at the SS4, but they bind only to NRXN-β variants (Siddiqui et al., 2010).

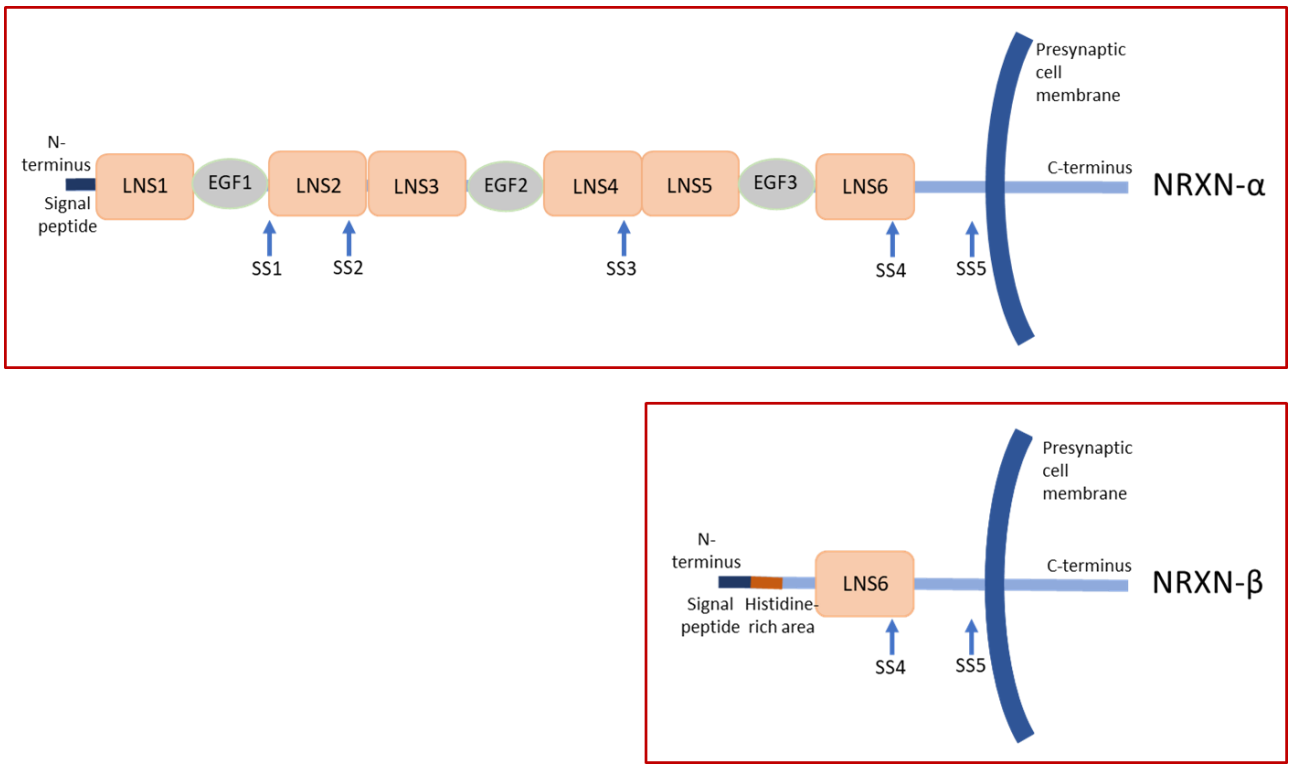

Figure 1.3 Domain Structures of Neurexins

NRXN-α extracellular region consists of a signal peptide, six LNS domains and three EGF domains. The domains in NRXN-α are arranged in sets of LNS-EGF-LNS repeated three times. NRXN-β extracellular part consists of a signal peptide, histidine-rich area and only one LNS domain which is similar to the sixth LNS domain of NRXN-α.

1.3 PREVIOUS STUDIES ABOUT THE INTERACTION BETWEEN CALSYNTENIN-3 AND NEUREXINS

Up to this point, there has been four studies published by two research groups about the interaction between CLSTN3 and NRXNs (Kim et al., 2020; Lu et al., 2014; Pettem et al., 2013; Um et al., 2014). However, all of these studies have contradicting claims about the interaction and the discrepancy remains to be resolved. Because the claims about the interaction between CLTN3 and NRXNs differ widely, the interaction might not get resolved before the structure of CLSTN3 is determined.

The first study (Pettem et al., 2013) that identified CLSTN3 as a NRXN specific binding partner claimed that CLSTN3 binds NRXN-α but does not bind NRXN-β. Pettem et al. also claimed that both the CAD domains and the LNS domain are necessary for the interaction. The interaction was also shown to be calcium dependent and the presence or the absence of the insert at SS4 in the NRXNs did not seem to have an effect on the interaction between CLSTN3 and NRXNs. The same group published their second article on the subject in 2014. In this study (Lu et al., 2014) they were able to confirm that the interaction between CLSTN3 and NRXN-α was mediated by the CLSTN3 LNS domain. They also showed that CLSTN3 ectodomain occurs as monomers and tetramers in solution and that both monomers and tetramers can bind NRXN-α. In this study Lu et al. also showed that the deletion of the sixth LNS domain of NRXN-α did not have an effect on the interaction.

Another group, Um et al. (2014), released a study briefly after the first study by Pettem et al. (2013). This study (Um et al., 2014) was not able to replicate the direct interaction between CLSNT3 and NRXN-α. Nevertheless, Um et al. found a functional connection between CLSTN3 and NRXNs. They also claimed that the synaptogenic activity of CLSTN3 was mediated by the CLSTN3 CAD domains and the LNS domain was not necessary for the synaptogenic activity (Um et al., 2014). The latest study (Kim et al., 2020) on the subject is from the same group as the second study (Um et al., 2014). In this study, Kim et al. (2020) claim that CLSTN3 CAD domains bind both NRXN-α and NRXN-β with a preference to SS4 positive NRXNs. Kim et al. also say that the LNS domain of the NRXN-β, which is identical to the sixth LNS domain of NRXN-α, is necessary for the interaction.

2. AIM OF THE STUDY

There is a discrepancy between the findings of Pettem et al. (2013) and Lu et al. (2014) and those of Um et al. (2014) and Kim et al. (2020), about the interaction between CLSTN3 and NRXNs. Therefore, the aim of this master's thesis study was to verify the binding domains of CLSTN3 in the interaction with NRXNs. The aim of this study was two-fold:

Firstly, the aim was to produce the CLSTN3 ectodomain protein constructs, that contain either the two CAD domains, the LNS domain or all three domains, using baculovirus mediated protein production in an insect cell culture. After which, the protein constructs were to be purified using affinity chromatography and size-exclusion chromatography.

Secondly, the aim of this study was to express the CLSTN3 ectodomain protein constructs on the surface of HEK293T cells and test the binding to NRXNs in a cell surface binding assay.

3. MATERIALS AND METHODS

3.1 BACULOVIRUS PRODUCTION AND PURIFICATION OF THE CLSTN3 ECTODOMAIN CONSTRUCTS

3.1.1 PRODUCTION OF THE RECOMBINANT BACULOVIRUSES

The five mouse CLSTN3 gene constructs, that are listed in Table 3.1, were cloned into modified p509.3 plasmid vector derived from the pFastBac1 expression vector (Keinänen et al., 1998). The expression constructs included the N-terminal honeybee melittin secretion signal sequence, the Flag-tag sequence and a C-terminal human IgG1 Fc (Fc) tag with a preceding PreScission protease (PSP) cleavage site. Four of the cloned constructs also included an N-terminal 6His tag. The CLSTN3 gene constructs were amplified, using PCR, from a CLSTN3 full ectodomain construct cloned into pDisplay vector, using appropriate forward and reverse primers for each construct. The primers were designed by doctoral student Sudeep Karki. Primers are listed in the Appendix 2. The PCR products and the p509.3_Fc plasmids were digested with FastDigest EcoRI and FastDigest BamHI (Thermo Scientific) restriction enzymes. The digested PCR products and plasmids were ligated with T4 DNA Ligase (Thermo Scientific).

Table 3.1 CLSTN3 Ectodomain Constructs That Were Cloned into p509.3_Fc

Construct	Amino acids	Fc tag	6His tag
CLSTN3_2CAD_LNS$_{6His_20\text{-}562_Fc}$	20 – 562	✓	✓
CLSTN3_2CAD_LNS$_{36\text{-}562_Fc}$	36 – 562	✓	✗
CLSTN3_2CAD$_{6His_20\text{-}259_Fc}$	20 – 259	✓	✓
CLSTN3_2CAD$_{6His_36\text{-}259_Fc}$	36 – 259	✓	✓
CLSTN3_LNS$_{6His_332\text{-}562_Fc}$	332 – 562	✓	✓

The plasmid constructs were transformed into competent *E.coli* XL10 Gold cells using heat shock transformation method (Froger and Hall, 2007). Briefly, the competent *E.coli* XL10 Gold cells (storage at -80 °C) were thawed on ice for 30 min. 10 µl of ligation mixture was added to a tube, containing 50 µl of thawed cells, and the tubes were incubated on ice for 30 min. Then the cells were given a heat shock at 42°C for 40 s immediately followed by an incubation on ice for 2 min. 500 µl of Super Optimal broth (SOC) was added to the tubes and the cells were grown at 37 °C for 1 hour, after which the cells were plated on Lysogeny broth (LB) agar plates, containing 100 µg/ml ampicillin and grown overnight at 37 °C. The next day, 4 ml cultures in LB media + 100 µg/ml ampicillin were started from individual colonies and the plasmids, containing the CLSTN3 ectodomain gene constructs were purified using GeneJET Plasmid Miniprep Kit (Thermo Scientific). The success of the cloning was confirmed by sequencing at Eurofins Genomics.

The recombinant bacmids, containing the mouse CLSTN3 gene constructs were generated by transforming the recombinant CLSTN3 p509.3_Fc plasmids into competent DH10EMBacY *E.coli* (Bac-to-Bac Baculovirus Expression System, 2015) using heat shock transformation method (Froger and Hall, 2007), as described above. After transformation the cells were grown in SOC media without antibiotics for overnight at 37 °C. The next day, the cells were plated on LB agar plates, containing 50 µg/ml kanamycin, 10 µg/ml tetracycline, 7 µg/ml gentamycin, 40 µg/ml IPTG and 100 µg/ml X-Gal, and the plates were incubated at 37 °C and white and blue colonies were obtained the next day. The blue colonies get their colour from the β-galactosidase activity of the DH10EMBacY *E.coli*, whereas the white colonies had lost the β-galactosidase activity, because of the insertion of the CLSTN3 gene constructs into the bacmid DNA (Bac-to-Bac Baculovirus Expression System, 2015). Seven white colonies and one blue colony, as a control, were picked from each plate, and re-plated on LB agar plates, containing 50 µg/ml kanamycin, 10 µg/ml tetracycline, 7 µg/ml gentamycin, 40 µg/ml IPTG and 100 µg/ml X-Gal. The next day, the colours of the colonies were confirmed. The presence of the CLSTN3 gene constructs in the bacmids was confirmed by PCR as described in the Bac-to-Bac Baculovirus Expression System manual (2015, p. 32). 4 ml cultures in LB media, containing 50 µg/ml kanamycin, 10 µg/ml tetracycline and 7 µg/ml gentamycin, were started from the confirmed positive colonies. The cultures were incubated for overnight at 37 °C and the recombinant bacmid DNA was extracted from the cultures.

The Sf9 cells, clonal isolates from the IPLB-Sf-21-AE *Spodoptera frugiperda* cell line, were seeded in CellStar (GreinerBio-one) 6-well plates 0.9 x 10^6 cells/well in HyClone SFX-Insect MP (SFX) insect cell

culture media (GE Healthcare). The Sf9 cells were transfected with the recombinant bacmids, using TransIT LT1 transfection reagent (Mirus). The transfected cells were grown at 27 °C for 4 – 7 days, and the cell growth was observed daily. After the majority of cells looked irregular and bigger than normally, which meant they were infected, the cells and the media were harvested as a suspension from the wells and these first recombinant virus stocks, called V_0, were stored in 15 ml falcon tubes at 4 °C in the dark. The second recombinant virus stocks, called V_1, were produced by adding 500 µl of V_0 to 20 ml Sf9 cell cultures in SFX media at live cell densities of 1.0 x 10^6 cells/ml and with cell viabilities over 95%, that were grown in Erlenmeyer flasks at 27 °C at a stirring rate of 90 rpm. The cell growth and viability of each culture was followed daily, and if the cell densities had exceeded 1.5 x 10^6 cells/ml, the cell cultures were diluted, using SFX media, back to 1.0 x 10^6 cells/ml. The infected cell suspensions were collected after 3 – 5 days, when the cell viability had decreased below 50%. These V_1 virus stocks were stored as 3 ml aliquots in 15 ml falcon tubes, that were flash-frozen in liquid nitrogen and stored at -80 °C.

The expression of the CLSTN3 ectodomain constructs in the Sf9 V_1 virus stocks was detected by western blotting. Briefly, 200 µl samples from each of the Sf9 V_1 virus stocks were centrifuged at 5000 rpm for 5 min, and the culture supernatants and the cell pellets were separated. The cell pellets were resuspended to 100 µl water. 10 µl of each supernatant and cell pellet samples were run on SDS-PAGE under reducing conditions. The proteins were transferred to polyvinylidene fluoride (PVDF) membranes, that were then blocked overnight in a tris-buffered saline (TBS) buffer containing 0.5% TWEEN® 20 (TBS-T) and 5% milk. The next day, the PVDF membranes were washed and incubated for 3 hours with Goat polyclonal antihuman IgG horseradish peroxidase-conjugated antibody (Abcam ab98567) diluted to 1:4000 in TBS-T with 1% milk. Then the PVDF membranes were washed with TBS-T and TBS, and incubated with Amersham ECL Select Western Blotting Detection Reagent (GE Healthcare) for 5 min. The expression was detected using the ChemiDoc XRS+ System (Bio-Rad).

3.1.2 PRODUCTION OF THE CLSTN3 ECTODOMAIN CONSTRUCTS IN HIGH FIVE CELL CULTURES

At first, the production of CLSTN3 ectodomain constructs was attempted in Sf9 cell cultures. In a nutshell, the Sf9 cell cultures were diluted in SFX media to live cell densities of 1.3 x 10^6 – 1.9 x 10^6 cells/ml at over 95% cell viability. The cell cultures were infected with the Sf9 V_1 virus stocks at the infection ratios of 1:200 or 1:1000. The cultures were grown in Erlenmeyer flasks at 27 °C at a stirring rate of 90 rpm for 72 hours. Then, the protein constructs were purified from the cell cultures in a similar manner that is described in the section 3.1.3. After the purification, the protein yields were measured, and the different infection ratios were compared against each other. The tested constructs and the protein yields are listed in the Appendix 3. For the constructs that had only little difference in the protein yield between the 1:200 or 1:1000 infection ratios, 1:500 infection ratio was decided to be used in the further experiments when comparing the expression in Sf9 and BTI-TN-5B1-4 *Trichoplusia ni* (High Five) cell cultures. Because the CLSTN3_2CAD$_{6His_20\text{-}259_Fc}$ V_1 virus stock was not tested in Sf9 cell cultures, 1:500 infection ratio was decided to be used in further experiments.

Because, the protein yields from the Sf9 cell cultures, expressing the CLSTN3 ectodomain constructs, was small, the CLSTN3 ectodomain constructs were decided to be produced in High Five cell cultures. Briefly, the High Five cell cultures were diluted in SFX media to live cell densities of 1.3 x 10^6 – 1.9 x 10^6 cells/ml at over 95% cell viability. The cell cultures were infected with the Sf9 V_1 virus stocks at the infection ratios of 1:200, 1:500 or 1:1000. The cultures were grown in Erlenmeyer flasks at 27 °C at a stirring rate of 90 rpm for 48 hours, 72 hours or 96 hours.

The optimal infection ratios and times were tested by infecting 5 ml cultures in SFX media with different infection ratios. The infection ratios that were used for Sf9 and High Five cell cultures are listed in Table 3.2. The optimal infection ratios and times were compared against the expression in Sf9 cell cultures. The infection ratios used for Sf9 cell cultures were based on the best infection ratios that were determined in the previous purification tests with Sf9 cell cultures, as discussed above. Samples from the Sf9 cell cultures were collected after 72 hours and samples from the High Five cell

cultures were collected after 48 hours, 72 hours and 96 hours. The workflow for testing the optimal infection ratio and time is displayed in Figure 3.2.

Table 3.2 Infection Ratios of the Sf9 and High Five Cell Cultures

V_1 virus stock	Infection Ratio			
	Sf9	High Five		
CLSTN3_2CAD_LNS$_{6His_20-562_Fc}$	1:200	1:200	1:500	1:1000
CLSTN3_2CAD_LNS$_{36-562_Fc}$	1:500	1:200	1:500	1:1000
CLSTN3_2CAD$_{6His_20-259_Fc}$	1:500	1:200	1:500	1:1000
CLSTN3_2CAD$_{6His_36-259_Fc}$	1:200	1:200	1:500	1:1000
CLSTN3_LNS$_{6His_332-562_Fc}$	1:500	1:200	1:500	1:1000

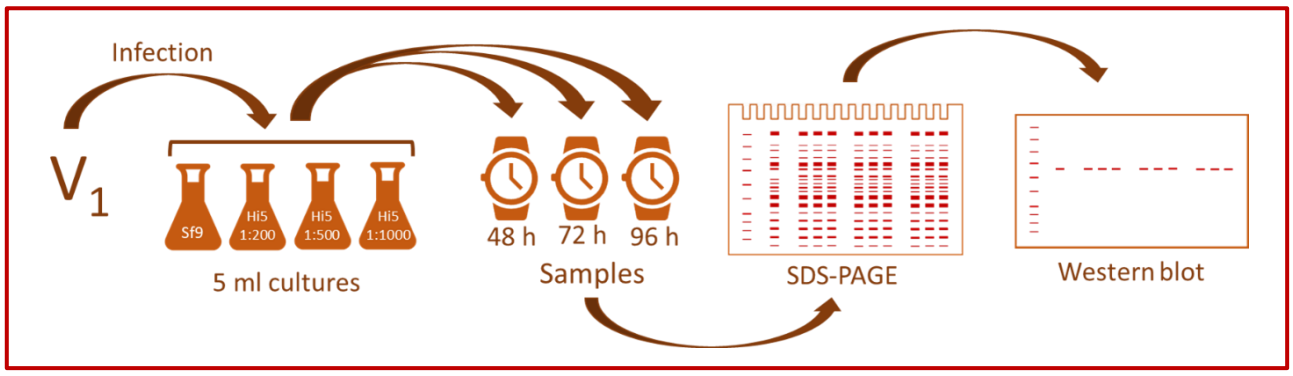

Figure 3.2 Workflow for Testing the Optimal Infection Ratio and Time

For each of the five CLSTN3 ectodomain constructs, four cell cultures were started: one Sf9 cell culture and three High Five cell cultures with different infection ratios. The 5 ml Sf9 and High Five cell cultures were infected using the Sf9 V_1 virus stocks at infection ratios that are listed in the Table 4.2. Samples were collected 48 h, 72 h and 96 h after the infection from each of the cell cultures. The cell culture samples were centrifuged at 5000 rpm for 5 min. The cell pellet was discarded, and the supernatant samples were stored at -20 °C. The supernatant samples were run on SDS-PAGE under reducing conditions and the western blotting was done as described above in the text.

After determining the optimal infection ratios and times for each of the Sf9 V_1 virus stocks when infecting High Five cell cultures, these optimal infection ratios and times were used in the subsequent High Five cell cultures. The expression levels were also compared between the different CLSTN3 ectodomain constructs. For the purification of the CLSTN3 ectodomain constructs, the Sf9 V_1 virus stocks that mediated the best expressions were selected for further use. The selected Sf9

V_1 recombinant viruses were: CLSTN3_2CAD_$LNS_{36\text{-}562_Fc}$, CLSTN3_$2CAD_{6His_36\text{-}259_Fc}$ and CLSTN3_$LNS_{6His_332\text{-}562_Fc}$. The CLSTN3 ectodomain constructs were purified from 50 – 400 ml High Five cell cultures.

3.1.3 PROTEIN-A AFFINITY PURIFICATION OF THE CLSTN3 ECTODOMAIN CONSTRUCTS

The secreted Fc-tagged CLSTN3 ectodomain constructs were purified from High Five cell culture supernatants. The High Five cell cultures were centrifuged at 7000 rpm at 4 °C for 30 min. The cell pellets were discarded, and the supernatants were filtered using 0.45 µm MF-Millipore Membrane Filters (Millipore). The affinity purification column, containing 1 ml protein-A sepharose (Invitrogen), was washed with 40 ml water and equilibrated with 20 ml binding buffer: 50 mM Tris-HCl pH 7.5, 300 mM NaCl and 5 mM $CaCl_2$. Then, the filtered supernatant was loaded to the column and the flow-through was collected. The flow-through was loaded onto the column again to ensure maximal binding of the Fc-tagged protein construct to the protein-A sepharose. The column was washed with 5 ml binding buffer to remove the unbound molecules from the column. The CLSTN3 ectodomain construct was eluted from the protein-A sepharose in ten 1-ml fractions, using 10 ml elution buffer: 100 mM glycine pH 3.0. The elution fractions were immediately neutralized into 60 mM Tris-HCl pH 7.5, 300 mM NaCl and 2 mM $CaCl_2$.

The amounts of purified proteins were calculated measuring the absorbance at 280 nm in the elution fraction tubes and dividing the absorbances by the absorbance coefficients of the constructs. The purified CLSTN3 ectodomain constructs were flash-frozen in liquid nitrogen and stored at -80 °C, or alternatively concentrated after addition of 10% glycerol, and prepared for the PreScission protease (PSP) cleavage. Only the CLSTN3_$LNS_{6His_332\text{-}562_Fc}$ ectodomain construct purification and concentration yielded enough protein to be cleaved and further purified using size-exclusion chromatography. The calculated CLSTN3_$LNS_{6His_332\text{-}562_Fc}$ protein yield was 3.64 mg.

3.1.4 PSP CLEAVAGE OF THE CLSTN3_LNS$_{6HIS_332\text{-}562_FC}$ CONSTRUCT AND THE SEPARATION OF THE FC TAG

The Fc-tagged CLSTN3_LNS$_{6His_332\text{-}562_Fc}$ ectodomain construct was cleaved using PSP. Briefly, the CLSTN3_LNS$_{6His_332\text{-}562_Fc}$ ectodomain construct was cleaved in cleavage buffer, containing 60 mM Tris-HCl pH 7.5, 300 mM NaCl, 2 mM $CaCl_2$, 0.1 mM DTT, 0.01% TWEEN® 20 and 10% glycerol. For each 1 mg of Fc-tagged CLSTN3_LNS$_{6His_332\text{-}562_Fc}$ ectodomain construct, 25 µg of PSP was added to the cleavage mixture. The mixture was incubated overnight at 4 °C.

The cleaved Fc tag was separated from the CLSTN3_LNS$_{6His_332\text{-}562}$ construct, using protein-A affinity chromatography. Briefly, the protein-A sepharose column was equilibrated with 20 ml wash buffer, containing 60 mM Tris-HCl pH 7.5, 300 mM NaCl and 2 mM $CaCl_2$. Then, the cleavage mixture was loaded to the column, and the mixture was incubated with the protein-A sepharose for 10 min. The column flow-through was collected and the loading and incubating was repeated two more times. Then the column flow-through was collected and stored and to collect any remaining CLSTN3_LNS$_{6His_332\text{-}562}$ construct from the protein-A sepharose, the column was washed with 5 ml wash buffer, containing 60 mM Tris-HCl pH 7.5, 300 mM NaCl and 2 mM $CaCl_2$ and the washing flow-through was collected. The column flow-through and the washing flow-through, containing the cleaved CLSTN3_LNS$_{6His_332\text{-}562}$ ectodomain construct, was flash-frozen in liquid nitrogen and stored in a falcon tube at -80 °C. The cleaved Fc tag was eluted from the protein-A sepharose column in 10 x 1ml fractions in elution buffer, containing 100 mM glycine pH 3. The elution fractions were immediately neutralized into 60 mM Tris-HCl pH 7.5 and 300 mM NaCl.

The efficiency of cleavage was verified using SDS-PAGE. Samples, taken from each step of the cleavage, were analysed by SDS-PAGE under reducing conditions. The efficiency of the cleavage was verified by comparing the samples taken before the cleavage, after the cleavage and after the separation of the CLSTN3_LNS$_{6His_332\text{-}562}$ ectodomain construct and the Fc tag.

3.1.5 SIZE-EXCLUSION CHROMATOGRAPHY OF THE CLSTN3_LNS$_{6HIS_332-562}$ ECTODOMAIN CONSTRUCT

The flow-through, containing the cleaved CLSTN3_LNS$_{6His_332-562}$ ectodomain construct, was concentrated to 500 µl. The sample contained 0.54 mg protein. The cleaved CLSTN3_LNS$_{6His_332-562}$ ectodomain construct sample was gel filtered with ÄKTA protein purification system, using Superdex 75 10/300 GL (GE Healthcare) in 60 mM Tris-HCl, 300 mM NaCl and 2 mM $CaCl_2$. A total of fifty 500 µl fractions were collected at 0.5 ml/min flowrate. The highest UV absorbance peak was observed in fractions 16 – 21. Size-exclusion chromatography (SEC) fractions 16 – 21 were collected and analysed using SDS-PAGE gel electrophoresis. The gel filtration profile is presented at Appendix 4. Samples were analysed by SDS-PAGE under reducing conditions.

The fractions 18 and 19, containing the SEC purified CLSTN3_LNS$_{6His_332-562}$ ectodomain construct, were pooled. The sample was concentrated to 100 µl, flash-frozen in liquid nitrogen and stored in an Eppendorf tube at -80 °C. Total protein yield after concentrating was 0.21 mg.

3.2 SEC-MALLS ANALYSIS OF THE CLSTN3_LNS$_{6HIS_332-562}$ ECTODOMAIN CONSTRUCT

The size-exclusion chromatography-coupled multi-angle static laser light scattering (SEC-MALLS) was done for the SEC purified CLSTN3_LNS$_{6His_332-562}$ ectodomain construct in 50 µl volume at 1.4 mg/ml concentration. The experiment was done at 0.5 ml/min flowrate in a buffer, containing 30 mM Tris-HCl pH 7.5, 150 mM NaCl and 2 mM $CaCl_2$, using HPLC system (Shimadzu) connected to a Superdex 200 10/300 (GE Healthcare) gel filtration column. The measurements were completed using a miniDAWN TREOS (Wyatt Technology Corporation) light scattering detector and an Optilab (Wyatt Technology Corporation) refractive index detector. The data was analysed using ASTRA 6 (Wyatt Technology Corporation) software.

3.3 BINDING ASSAY OF THE CELL SURFACE EXPRESSED CLSTN3 AND THE SOLUBLE NRXN VARIANTS

3.3.1 EXPRESSION OF THE CLSTN3 ECTODOMAIN CONSTRUCTS IN HEK293T CELLS

The four mouse CLSTN3 gene constructs, that are listed in Table 3.3, were cloned, in a similar manner that was described in the section 3.1.1, into pDisplay mammalian expression vectors, containing an ampicillin resistance gene, an N-terminal signal sequence followed by an HA tag, and the C-terminal Myc tag followed by PDGFR transmembrane domain. The restriction enzymes, used in the digestion of the PCR products and the pDisplay vector, were FastDigest SmaI and FastDigest SalI (Thermo Scientific). The recombinant CLSTN3 pDisplay plasmids were produced in *E.coli* XL10 Gold cells and purified similarly as described in the section 3.1.1. The cloning results were verified by sequencing at Eurofins Genomics.

Table 3.3 CLSTN3 Ectodomain Constructs That Were Cloned into pDisplay

Construct	Amino acids	HA tag
CLSTN3_Full ectodomain$_{20\text{-}847}$_pDisplay	20 – 847	✓
CLSTN3_2CAD_LNS$_{20\text{-}562}$_pDisplay	20 – 562	✓
CLSTN3_2CAD$_{20\text{-}259}$_pDisplay	20 – 259	✓
CLSTN3_LNS$_{332\text{-}562}$_pDisplay	332 – 562	✓

The recombinant CLSTN3 ectodomain constructs were expressed in human embryonic kidney 293T (HEK293T) cells. Briefly, 25 000 HEK293T cells/well in 0.5% fetal bovine serum (FBS) supplemented Dulbecco's Modified Eagle's medium (DMEM) pH 7.4 media (DMEM+FBS) were plated into sterile 96-well plates, that were coated with poly-L-lysine for 1 hour. The plates were incubated at 37 °C in 5% CO_2 for 24 hours and the DMEM+FBS media were changed to fresh DMEM+FBS media. The HEK293T cells were transiently transfected with the recombinant CLSTN3 pDisplay plasmids using

400 ng or 700 ng of plasmid/well combined to 1200 ng or 2800 ng polyethyleneimine (PEI), respectively, with ratio of DNA/PEI of 1/3. After transfection, the plates were incubated at 37 °C in 5% CO_2 for 3 hours. The DMEM+FBS media were changed to fresh DMEM+FBS media and the plates were incubated in 37 °C 5% CO_2 incubator for 72 hours. The complete workflow of the transient transfection is illustrated in Figure 3.3.

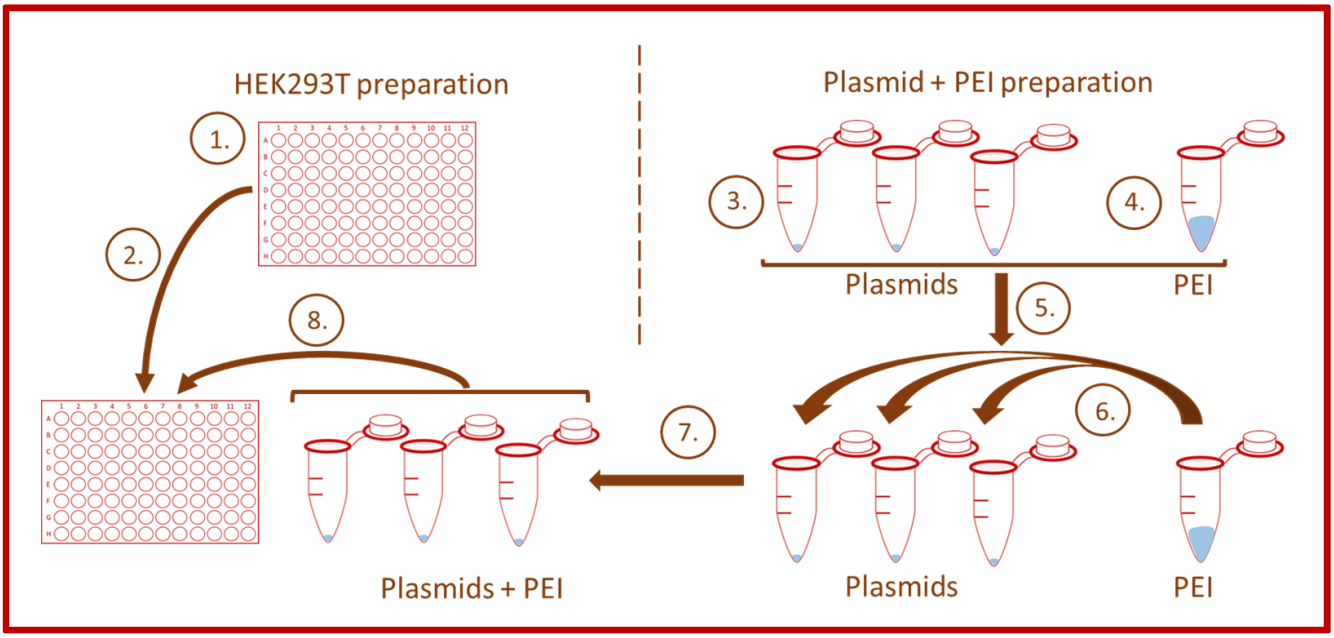

Figure 3.3 Transient Transfection Workflow

1. The DMEM+FBS media was changed in the wells containing the HEK293T cells. 2. The plates were incubated in room temperature until the plasmids were prepared. 3. The plasmid DNA was diluted to 10 µl/well DMEM+FBS. 4. The PEI was diluted to 10 µl/well DMEM+FBS. 5. The plasmid DNA and PEI solutions were incubated at room temperature for 5 min. 6. 10 µl of PEI solution was added to 10 µl of plasmid DNA solution. 7. The plasmid + PEI solutions were incubated at room temperature for 25 min. 8. 20 µl of the plasmid + PEI solutions were added to the wells.

The expression of the recombinant CLSTN3 ectodomain constructs in HEK293T cells was verified by immunofluorescence. Briefly, the transfected cells grown in the 96-well plates were washed with 100 µl phosphate-buffered saline (PBS) and fixed with 50 µl 4 % paraformaldehyde (PFA) in PBS for 20 min. Then the wells, containing fixed cells, were blocked in 50 µl 1% bovine serum albumin (BSA) in PBS for 1 – 2 hours. The primary antibody (Anti-HA Rabbit, Santa Cruz) diluted to 1:300 in 50 µl PBS was added to the wells followed by a 1-hour incubation. The wells were washed with 100 µl PBS and the secondary antibody (Alexa488-anti-Rabbit, Molecular probes) diluted to 1:500 in PBS was added to the wells followed by a 1-hour incubation. The cells were washed three times with 100 µl PBS and imaged, using FLoid Cell Imaging system, using green light.

3.3.2 CELL SURFACE BINDING ASSAY

For the cell surface binding assay, the HEK293T cells in 96-well plates were transfected with the recombinant pDisplay CLSTN3 ectodomain plasmids as described in section 3.3.1. The cell surface binding assay was performed 72 hours after the transfection. To find out which NRXN variant CLSTN3 binds to, the binding assay was performed with three different NRXN variants: NRXN-1α_{Fc}, NRXN-1β_{GST} with the fourth splice site (+SS4) and NRXN-1β_{GST} without the fourth splice site (-SS4). The NRXN-1β_{GST} variants carried a glutathione-s-transferase (GST) affinity tag and the NRXN-1α_{Fc} carried an Fc tag. The workflow of the cell surface binding assay for both the NRXN-1β_{GST} variants and NRXN-1α_{Fc} against the CLSTN3 ectodomain constructs expressed on the surface of the HEK293T cells is presented in the Figure 3.4.

For the cell surface binding assay, the HEK293T cells in 96-well plates were washed twice with 50 µl PBS and fixed with 50 µl 4% PFA in PBS for 20 min in room temperature. After that, the wells were washed with 50 µl PBS and blocked for 3 hours in room temperature in 300 µl blocking buffer: 10 mM HEPES pH 7.2, 168 mM NaCl, 2.6 mM KCl, 2 mM $CaCl_2$, 2 mM $MgCl_2$, 10 mM D-glucose and 5% BSA. Then, the wells were washed with 50 µl EGB buffer: 10 mM HEPES pH 7.2, 168 mM NaCl, 2.6 mM KCl, 2 mM $CaCl_2$, 2 mM $MgCl_2$, 10 mM D-glucose and 1% BSA (Siddiqui et al., 2013). Then, one of the following was added to the wells: NRXN-1α_{Fc} diluted to 0.8 µM concentration in 50 µl EGB buffer, NRXN-1β_{GST}(+SS4) diluted to 1 µM concentration in 50 µl EGB buffer or NRXN-1β_{GST}(-SS4) diluted to 1 µM concentration in 50 µl EGB buffer, following an incubation at the room temperature for overnight.

For the plates incubated with the NRXN-1β_{GST}(+SS4) or NRXN-1β_{GST}(-SS4), incubations with both primary and secondary antibody were necessary, because the primary antibody (Rabbit-anti-GST) bound to the GST tag and the secondary antibody (IRDye® 680RD Goat anti-Rabbit IgG, LI-COR) bound to the primary antibody. Thus, the next day, the wells in the plates were washed three times with 100 µl EGB buffer followed by addition of primary antibody (Rabbit-anti-GST) diluted 1:500 in 50 µl EGB buffer and an incubation for 1 hour at room temperature. Next, the wells were washed three times with 100 µl EGB buffer followed by addition of the secondary antibody (IRDye 680RD Goat anti-Rabbit IgG, LI-COR) diluted 1:200 in 50 µl EGB buffer and an incubation for 1 hour at room temperature. Finally, the wells were washed three times with 100 µl TBS and dried for 10 minutes

lid open at room temperature. The binding of the NRXN-1β_{GST}(+SS4) and NRXN-1β_{GST}(-SS4) to the HEK293T cells expressing the CLSTN3 ectodomain constructs was detected with LI-COR Odyssey imaging system using the 700 nm channel at scan intensity 3 – 5, 169 µm pixel size and at both medium and highest quality.

For the plates incubated with the NRXN-1α_{Fc}, incubations with only the secondary antibody was necessary, because the secondary antibody (IRDye 800CW Goat anti-Human IgG, LI-COR) bound to the Fc tag. Accordingly, the next day, the wells in the plates were washed three times with 100 µl EGB buffer followed by addition of the secondary antibody (IRDye 800CW Goat anti-Human IgG, LI-COR) diluted 1:200 in 50 µl EGB buffer to the wells and incubation for 1 hour at room temperature. Lastly, the wells were washed three times with 100 µl TBS and dried for 10 minutes lid open at room temperature. The binding of the NRXN-1α_{Fc} to the HEK293T cells expressing the CLSTN3 ectodomain constructs was detected with LI-COR Odyssey imaging system using the 800 nm channel at scan intensity 5, 169 µm pixel size and at both medium and highest quality.

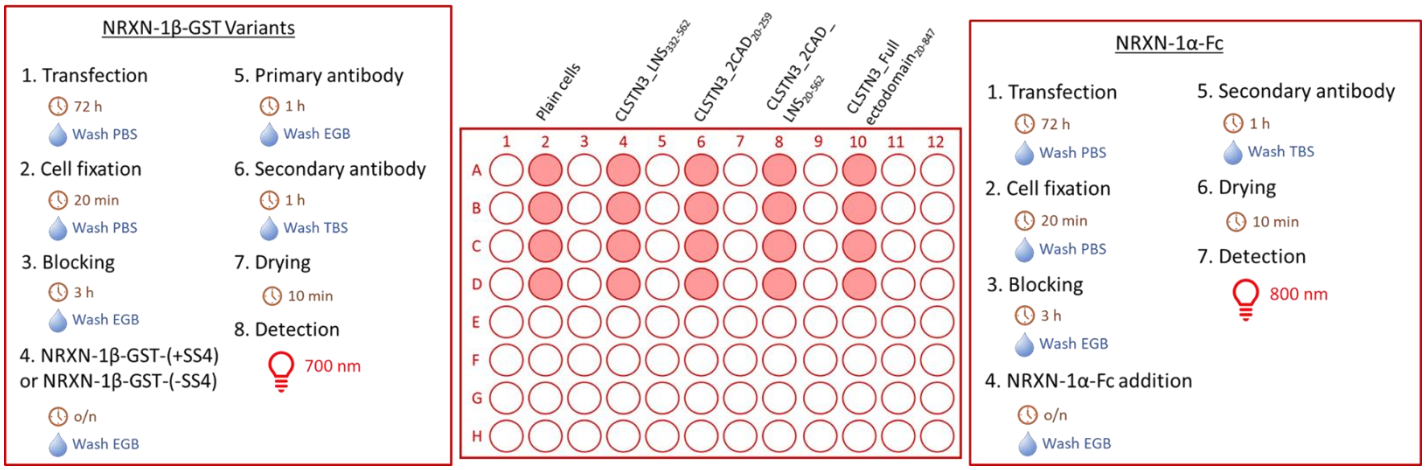

Figure 3.4 The Workflow of the Cell Surface Binding Assay

The CLSTN3 ectodomain constructs were expressed on the surface of the HEK293T cells, that were grown in 96-well plates. Each construct was expressed either in three or four wells. As a control, also triplicates or quadruplicates of wells, containing cells that did not express any of the CLSTN3 ectodomain constructs (plain cells), were grown on the plates. The binding assay against the NRXN-1β_{GST}(+SS4) and the NRXN-1β_{GST}(-SS4) was done according to the workflow presented on the left side of the figure. The binding assay against the NRXN-1α_{Fc} was done according to the workflow presented on the right side of the figure.

4. RESULTS

4.1 PRODUCTION AND PURIFICATION OF CLSTN3 ECTODOMAIN CONSTRUCTS

4.1.1 CLSTN3 ECTODOMAIN CONSTRUCTS HAD EXPRESSION IN BOTH SF9 AND HIGH FIVE CELL CULTURES

The viruses, carrying the CLSTN3 ectodomain construct DNA, were produced in the Sf9 cell cultures and the protein construct expression in the V_1 virus stocks was analysed by western blotting, which is presented in Figure 4.1. For four of the constructs two separate V_1 virus stocks were tested for expression and for the CLSTN3_2CAD$_{6His_20\text{-}259_Fc}$ construct only one V_1 virus stock was tested. All of the virus stocks had protein expression and the differences between the two virus stocks, expressing the same construct, were small. Therefore, the first V_1 stock, of all constructs, was decided to be used in the following protein purification experiments.

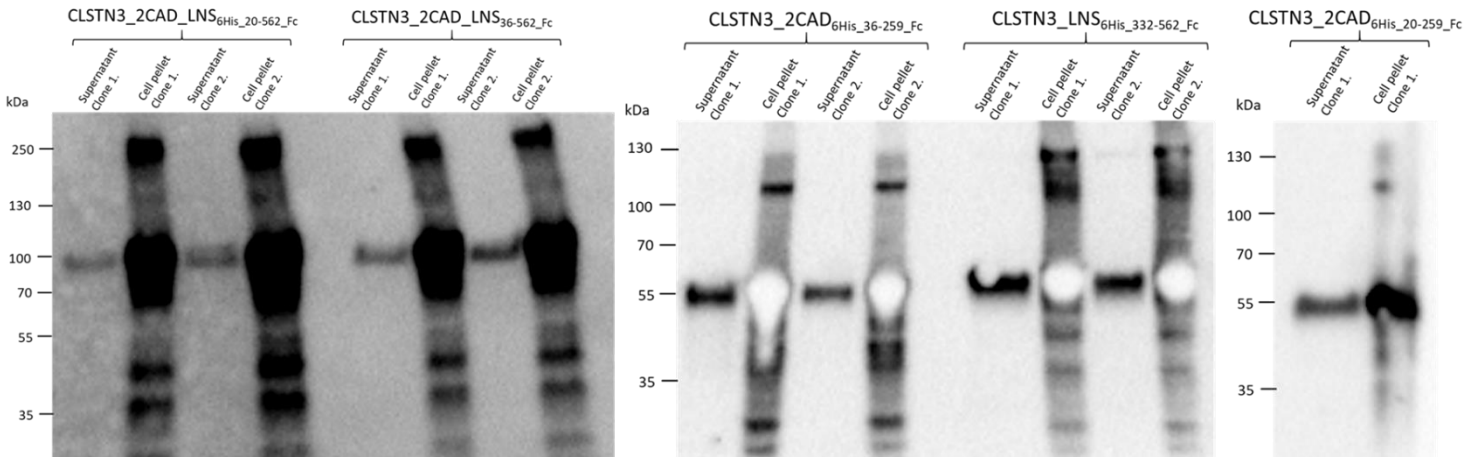

Figure 4.1 Expression of the CLSTN3 Ectodomain Constructs in the Sf9 V_1 Virus Stocks

For four of the constructs, two V_1 virus stocks (clones 1. and 2.) were tested, and for the CLSTN3_2CAD$_{6His_20\text{-}259}$ only one V_1 virus stock was tested. All V_1 virus stocks had expression in the supernatant. The cell pellets also showed a lot of expression which indicates that all of the protein was not secreted out of the Sf9 cells.

At first, the production of the CLSTN3 ectodomain constructs was attempted in Sf9 cell cultures. The protein yields from the Sf9 cell cultures were small (Appendix 3) regardless that different infection ratios were tested. Therefore, the High Five cell cultures were decided to be tested to gain an improved protein yield, as has been observed when comparing Sf9 and High Five cells (Wilde et al., 2014). The optimal infection ratio and time in High five cell cultures were determined by initiating three High five test cultures with different infection ratios and one Sf9 test culture for comparison. Samples were collected from the High Five cell cultures at certain timepoints after infection with the V1 virus stock and analysed by western blotting. In all of the constructs the expression in High five cell cultures were higher or at least in the same level as in the Sf9 cell cultures. For all constructs the 1:200 infection ratio was found to give the best expression and the optimal time to harvest the cells after infection was found to be 72 h. The western blot results are presented in the Figure 4.2. The constructs that had the best expression in the High Five cell cultures and that were decided to be used for protein purification from the bigger cultures were CLSTN3_2CAD_LNS$_{36\text{-}562_Fc}$, CLSTN3_2CAD$_{6His_36\text{-}259_Fc}$ and CLSTN3_LNS$_{6His_332\text{-}562_Fc}$.

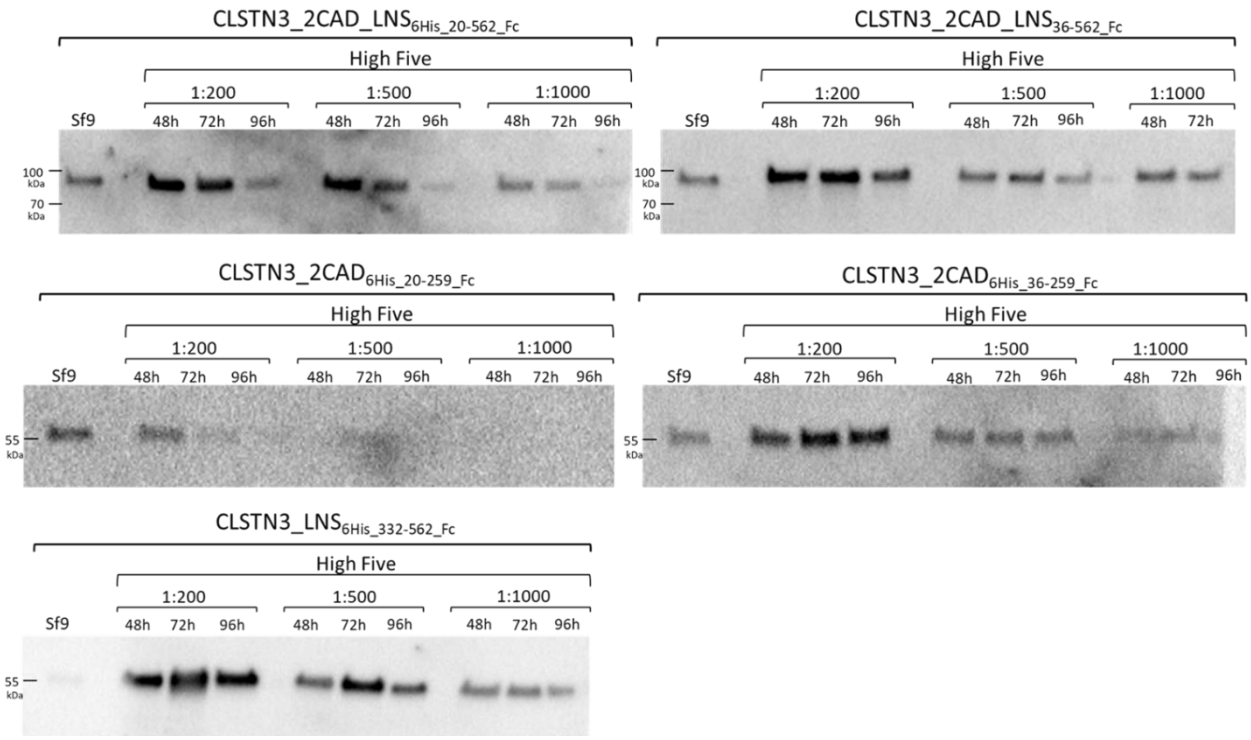

Figure 4.2 Optimal Infection Ratios and Times in High Five Cell Cultures

The optimal infection ratio was determined by comparing the protein expression in the samples taken from the cultures that were infected with different amounts of the V_1 virus stock. The optimal time for harvesting after the infection was determined by comparing the samples taken at different time points after the infection. The expression in High five cell cultures were also compared to the expression in the Sf9 cell cultures. The 1:200 infection ratio and the 72-hour infection time was found to be the best from the times and infection ratios that were tested for all of the constructs.

4.1.2 PURIFICATION OF CLSTN3_LNS$_{6HIS_332\text{-}562_FC}$ YIELDED ENOUGH PROTEIN TO BE USED IN FURTHER EXPERIMENTS

CLSTN3_2CAD_LNS$_{36\text{-}562_Fc}$, CLSTN3_2CAD$_{6His_36\text{-}259_Fc}$ and CLSTN3_LNS$_{6His_332\text{-}562_Fc}$ ectodomain constructs were produced in High five cell cultures. The protein yields, culture volumes and absorbances from the affinity purifications are listed in the Table 4.1. The CLSTN3_2CAD_LNS$_{36\text{-}562_Fc}$ and CLSTN3_2CAD$_{6His_36\text{-}259_Fc}$ were produced in 50 ml and 100 ml cultures, respectively. The calculated protein yields from the affinity purifications of these cultures were 0.62 mg and 1.09 mg, respectively. However, because the A260/A280 ratio was very high in the elution fractions from both of these affinity purifications, the actual protein yields were likely to be smaller than the calculated protein yields (Manchester, 1996). The elution fractions from the affinity purifications were concentrated to get a better understanding of the actual protein yield. After the concentration, the samples had very little to no protein left in them. Despite several attempts, these protein constructs did not yield enough protein to be used in the future experiments.

CLSTN3_LNS$_{6His_332\text{-}562_Fc}$ was produced in 400 ml High five cell culture. The calculated protein yield from the affinity purification was 3.64 mg. The A260/A280 was 0.68, which indicates that the sample had good quality, little nucleic acid contamination and therefore the calculated protein yield was likely to be near the correct value (Manchester, 1996). The sample had enough protein so it could be cleaved with the PSP.

Table 4.1 Protein yield table after the affinity purification

Construct	CLSTN3_2CAD_LNS$_{36\text{-}562_Fc}$	CLSTN3_2CAD$_{6His_36\text{-}259_Fc}$	CLSTN3_LNS$_{6His_332\text{-}562_Fc}$
Culture volume	50 ml	100 ml	400 ml
Volume of the elution fractions that included the purified protein	5 ml	5 ml	10 ml
Absorbance at 260 nm	0.239	0.349	0.390
Absorbance at 280 nm	0.182	0.263	0.572
A260/A280	1.31	1.33	0.68
Calculated protein yield	0.62 mg	1.09 mg	3.64 mg

CLSTN3_LNS$_{6His_332-562_Fc}$ ectodomain construct including the Fc tag was cleaved with PSP to separate the Fc tag from the CLSTN3_LNS$_{6His_332-562}$ ectodomain construct. The cleavage was performed twice, because after the first PSP cleavage there was still some uncleaved protein in the sample. Before the first cleavage the amount of uncleaved protein was 3.64 mg in 10 ml volume and after the first cleavage the amount of cleaved protein was 1.02 mg. After the first cleavage the sample, that included the uncleaved protein and the Fc tag, was concentrated to 5 ml and the cleavage was performed again. After the second cleavage, the total amount of cleaved CLSTN3_LNS$_{6His_332-562}$ was 1.38 mg in 15 ml volume. The cleaved protein sample was concentrated to 0.5 ml in which the final protein yield was 0.54 mg of cleaved CLSTN3_LNS$_{6His_332-562.}$ The samples taken at each step of the cleavage were analysed by SDS-PAGE, which is presented in the Figure 4.3. The amounts of cleaved and uncleaved protein before and after the first and the second cleavage are listed in the Table 4.2.

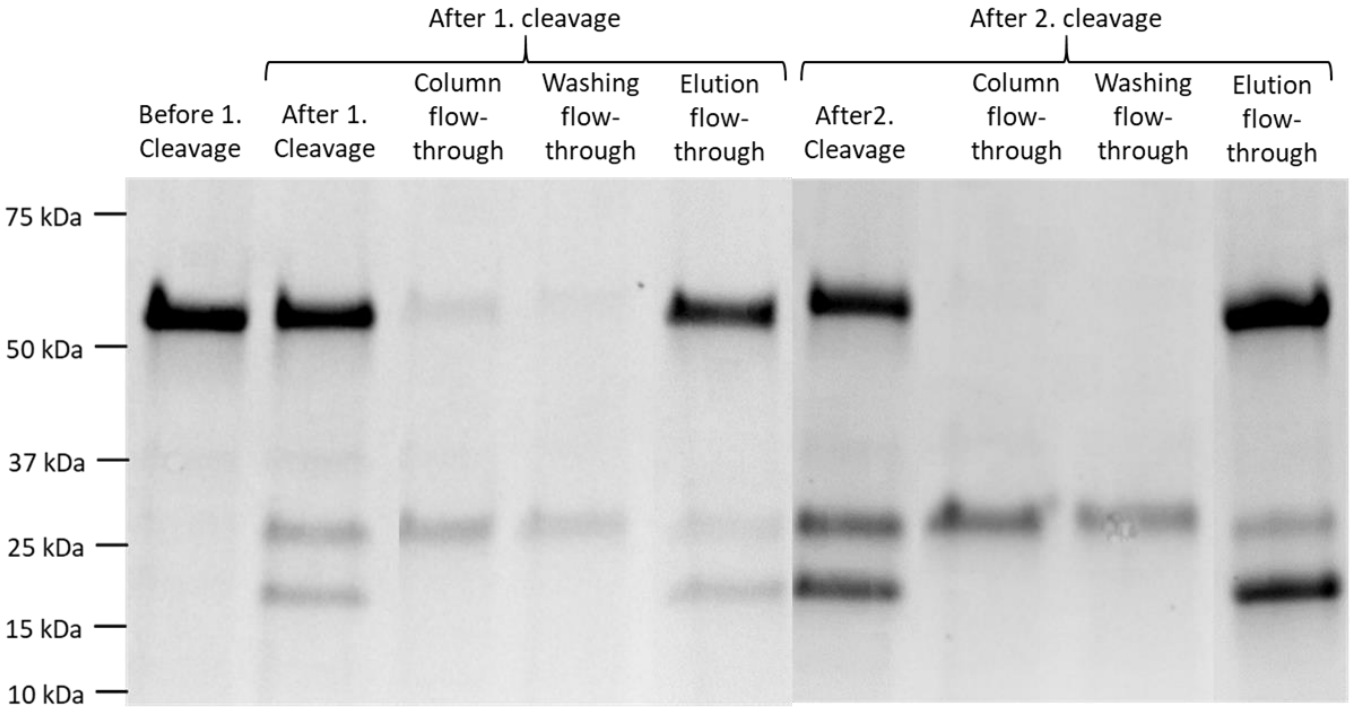

Figure 4.3 SDS-Page picture from the PSP cleavage of CLSTN3_LNS$_{6His_332-562_Fc}$

Samples were collected before and after the first and the second cleavage and analysed by SDS-PAGE. Before the first cleavage, the sample included only the uncleaved CLSTN3_LNS$_{6His_332-562_Fc}$ protein construct. After the first cleavage the sample had some uncleaved protein, the cleaved CLSTN3_LNS$_{6His_332-562}$ protein construct and the cleaved Fc tag. During the separation of the CLSTN3_LNS$_{6His_332-562}$ and the Fc tag, the CLSTN3_LNS$_{6His_332-562}$ did not bind to the protein-A matrix while the Fc tag and the uncleaved CLSTN3_LNS$_{6His_332-562_Fc}$ bound to the matrix. Therefore, the CLSTN3_LNS$_{6His_332-562}$ was in the column flow-through and the washing flow-through, and the elution flow-through included the Fc tag and the uncleaved CLSTN3_LNS$_{6His_332-562_Fc}$. The elution flow-through from the first cleavage was cleaved again and the samples after the second cleavage were also collected. For the final sample that included the cleaved CLSTN3_LNS$_{6His_332-562}$, the column flow-throughs from both cleavages were pooled and concentrated.

Table 4.2 Protein yield during the PSP cleavage

	Before 1. cleavage	After 1. cleavage/before 2. cleavage	After 2. cleavage	After concentrating
Amount of uncleaved protein (A260/A280)	3.64 mg (0.68)	1.91 mg (0.60)	1.28 mg (0.61)	—
Amount of cleaved protein (A260/A280)	—	1.02 mg (0.96)	1.02 mg + 0.36 mg = 1.38 mg (0.91)	0.54 mg (0.68)

After the cleavage the CLSTN3_LNS$_{6His_332-562}$ sample was filtered using SEC. The gel-filtration profile is presented in the Appendix 4. The CLSTN3_LNS$_{6His_332-562}$ protein was eluted to fractions 16. – 21. and these fractions were analysed by SDS-PAGE, which is presented in the Figure 4.4. The fractions 18. and 19. were pooled and the 1 ml sample contained 0.21 mg protein. The sample was concentrated to 0.1 ml. After concentration the sample included 0.14 mg protein and the protein concentration was 1.4 mg/ml.

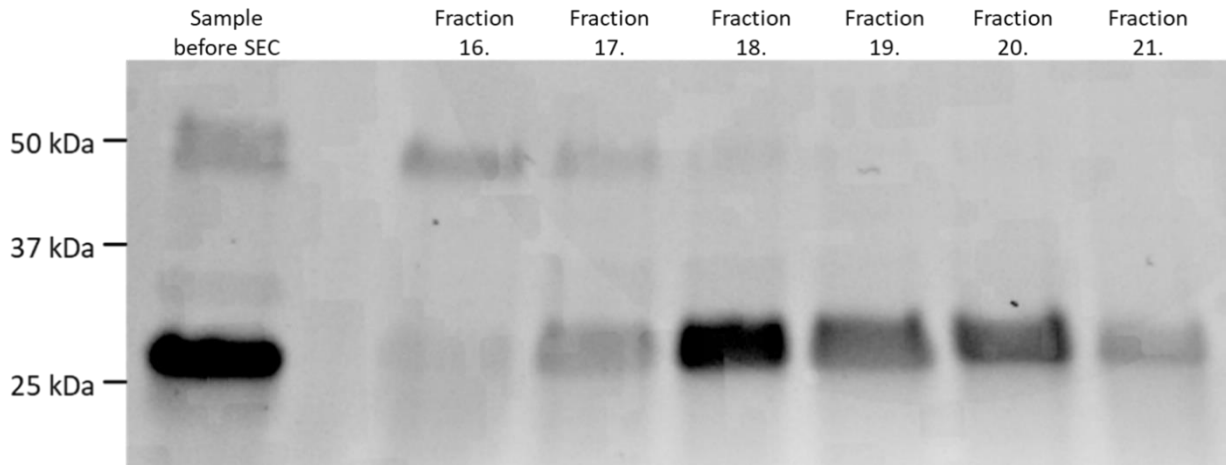

Figure 4.4 SDS-PAGE of SEC Fractions 16 – 21

The SEC fractions that included the protein were analysed by SDS-PAGE. The sample before SEC contained the CLSTN3_LNS$_{6His_332-562}$ and some uncleaved CLSTN3_LNS$_{6His_332-562_Fc}$. The fractions 16. and 17. included mostly the uncleaved CLSTN3_LNS$_{6His_332-562_Fc}$. The fractions 18. – 21. included the cleaved CLSTN3_LNS$_{6His_332-562}$.

4.2 CLSTN3_LNS$_{6HIS_332-562}$ FORMS DIMERS IN SOLUTION

The SEC-MALLS analysis revealed that CLSTN3_LNS$_{6His_332-562}$ forms dimers in solution. The observed molecular weight from the SEC-MALLS measurement was 68.8 kDa. The result is presented in the Figure 4.5. The calculated molecular weight of the CLSTN3_LNS$_{6His_332-562}$ monomer is 29.4 kDa and it has two N-linked glycosylation sites. In insect cells the N-linked glycans that are post-translationally added to the proteins are paucimannosidic glycans or oligomannosidic glycans that have a size of 1 – 2 kDa (Shi and Jarvis, 2007). However, in SEC-MALLS measurements the glycans contribute about 3 – 5 kDa to the protein molecular weight, because several factors affect the elution rate of the protein in the SEC and the SEC-MALLS is optimized only for proteins and not glycans or other molecules (Wang et al., 2017)

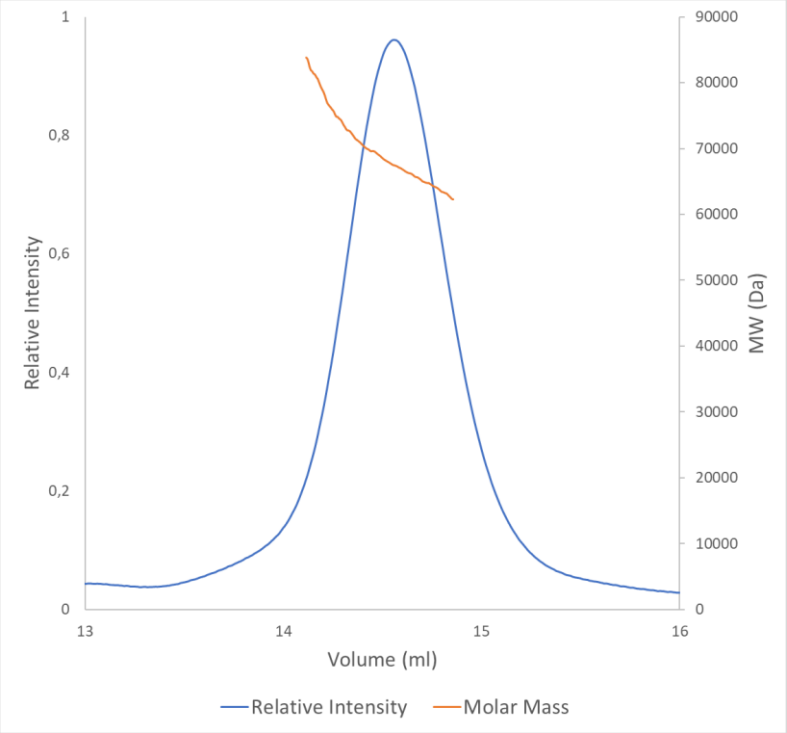

Figure 4.5 SEC-MALLS Analysis of the CLSTN3_LNS$_{6His_332-562}$ Oligomerization

The CLSTN3_LNS$_{6His_332-562}$ eluted from the SEC column at volume 14 – 15 ml and the measured molecular weight was 68.8 kDa.

4.3 EXPRESSION OF THE CLSTN3 ECTODOMAIN CONSTRUCTS ON THE SURFACE OF THE HEK293T CELLS AND THE CELL SURFACE BINDING ASSAY

4.3.1 CLSTN3 ECTODOMAIN CONSTRUCTS WERE EXPRESSED ON THE SURFACE OF THE HEK293T CELLS

The CLSTN3 ectodomain constructs CLSTN3_Full ectodomain$_{20\text{-}847}$, CLSTN3_2CAD_LNS$_{20\text{-}562}$, CLSTN3_2CAD$_{20\text{-}259}$ and CLSTN3_LNS$_{332\text{-}562}$ were expressed on the surface of the HEK293T cells and the expression was verified by immunofluorescence. All of the constructs had expression on the surface of the HEK293T cells. The fluorescent images are presented in the Figure 4.6.

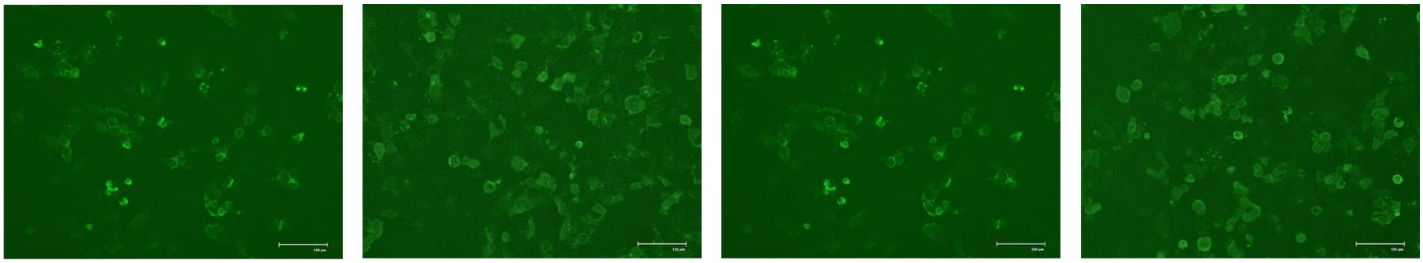

Figure 4.6 CLSTN3 Ectodomain Construct Expression on the Surface of the HEK293T Cells

CLSTN3_Full ectodomain$_{20\text{-}847}$, CLSTN3_2CAD_LNS$_{20\text{-}562}$, CLSTN3_2CAD$_{20\text{-}259}$ and CLSTN3_LNS$_{332\text{-}562}$ expression on the surface of the HEK293T cells was verified by immunofluorescence.

4.3.2 CLSTN3 CADHERIN DOMAINS BIND NRXN-1α

The interaction between the CLSTN3 ectodomain constructs expressed on the surface of the HEK293T cells and the NRXN variants NRXN-1α$_{Fc,}$ NRXN-1β$_{GST}$(+SS4) and NRXN-1β$_{GST}$(-SS4) was tested in a cell surface binding assay. The signal intensity was measured in the wells and compared

against the negative control that did not have expression of any CLSTN3 ectodomain construct on the surface of the HEK293T cells in the wells.

The cell surface binding assay showed that NRXN-1α_{Fc} bound to CLSTN3_2CAD$_{20\text{-}259}$ and CLSTN3_2CAD_LNS$_{20\text{-}562}$ but did not bind to CLSTN3_LNS$_{332\text{-}562}$ or CLSTN3_Full ectodomain$_{20\text{-}847}$ as compared to the negative control. This suggests that NRXN-1α_{Fc} binds to CLSTN3 cadherin domains but does not bind to the LNS domain. However, the result was contradicting because NRXN-1α_{Fc} did not bind to the CLSTN3_Full ectodomain$_{20\text{-}847}$, which suggests that CLSTN3 does not bind NRXN-1α_{Fc}. Nevertheless, NRXN-1α_{Fc} bound to CLSTN3_2CAD_LNS$_{20\text{-}562}$ but the measured signal intensity was lower than the signal intensity in the wells expressing CLSTN3_2CAD$_{20\text{-}259}$. The interaction between the CLSTN3 ectodomain constructs and the NRXN-1α_{Fc} in the cell surface binding assay is presented in the Figure 4.7.

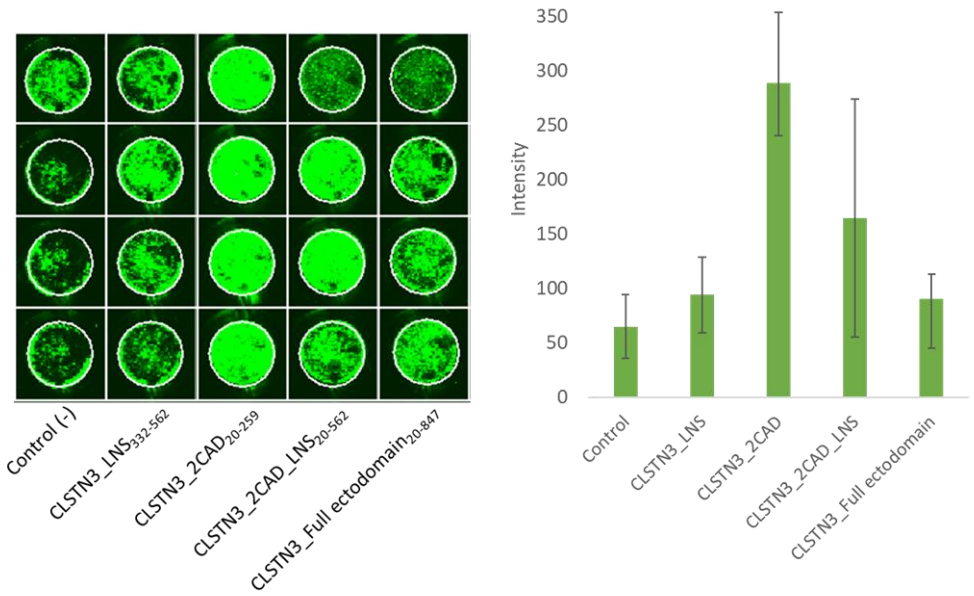

Figure 4.7 Interaction between the CLSTN3 Ectodomain Constructs and the NRXN-1α_{Fc}

The signal intensity of the interaction between the CLSTN3 ectodomain constructs and the NRXN-1α_{Fc} was compared to the negative control with intensity of 64. The signal intensities of the interaction between the NRXN-1α_{Fc} and the CLSTN3 ectodomain constructs: CLSTN3_LNS$_{332\text{-}562}$, CLSTN3_2CAD$_{20\text{-}259}$, CLSTN3_2CAD_LNS$_{20\text{-}562}$ and CLSTN3_Full ectodomain$_{20\text{-}847}$ were 94, 289, 165 and 90, respectively.

The cell surface binding assay did not show interaction between the CLSTN3 ectodomain constructs and the NRXN-1β_{GST}(-SS4) nor the NRXN-1β_{GST}(+SS4) as compared to the negative control. When testing the interaction between the CLSTN3 ectodomain constructs and the NRXN-1β_{GST}(-SS4), the measured signal intensities of the wells, expressing CLSTN3_LNS$_{332\text{-}562}$, CLSTN3_2CAD$_{20\text{-}259}$ and

CLSTN3_2CAD_LNS$_{20\text{-}562}$, were similar to the signal intensity of the negative control. Only the wells expressing the CLSTN3_Full ectodomain$_{20\text{-}847}$ had slightly higher signal intensity than the negative control. Also, when testing the interaction between the CLSTN3 ectodomain constructs and the NRXN-1β$_{GST}$(+SS4), the measured signal intensities in all of the wells were similar to the signal intensity of the negative control. These results suggest that CLSTN3 does not bind to NRXN-1β$_{GST}$(-SS4) or NRXN-1β$_{GST}$(+SS4). The results from the cell surface binding assays are presented in the Figure 4.8.

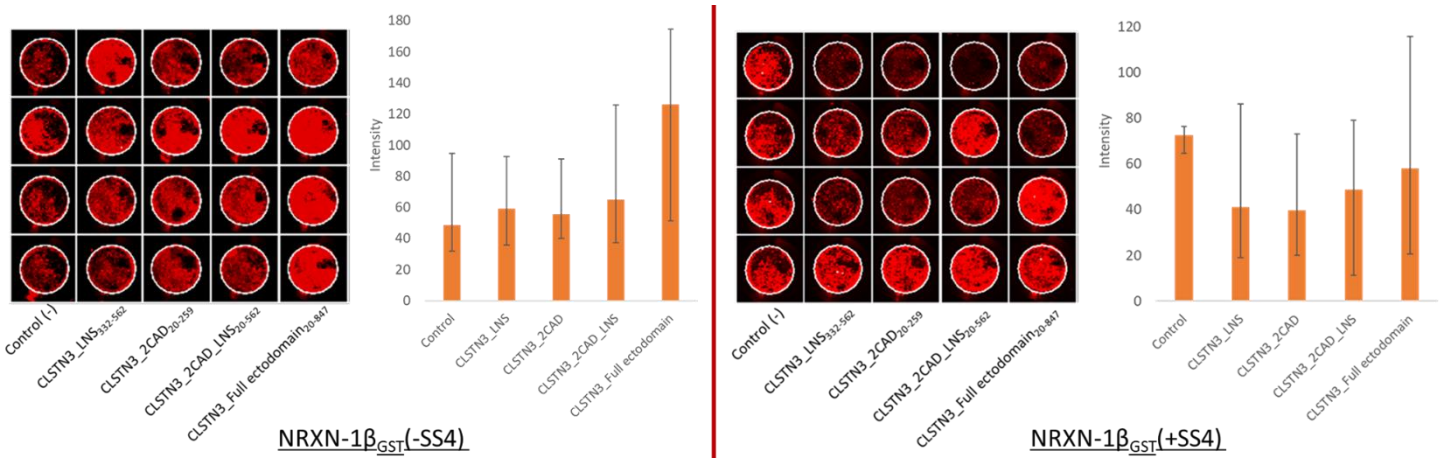

Figure 4.8 Interaction between the CLSTN3 Ectodomain Constructs and the NRXN-1β$_{GST}$(-SS4) and NRXN-1β$_{GST}$(+SS4)

On the left: The signal intensity of the interaction between the CLSTN3 ectodomain constructs and the NRXN-1β$_{GST}$(-SS4) was compared to the negative control with intensity of 49. The signal intensities of the interaction between the NRXN-1β$_{GST}$(-SS4) and the CLSTN3 ectodomain constructs: CLSTN3_LNS$_{332\text{-}562}$, CLSTN3_2CAD$_{20\text{-}259}$, CLSTN3_2CAD_LNS$_{20\text{-}562}$ and CLSTN3_Full ectodomain$_{20\text{-}847}$ were 59, 56, 65 and 126, respectively. **On the right:** The signal intensity of the interaction between the CLSTN3 ectodomain constructs and the NRXN-1β$_{GST}$(+SS4) was compared to the negative control with intensity of 73. The signal intensities of the interaction between the NRXN-1β$_{GST}$(+SS4) and the CLSTN3 ectodomain constructs: CLSTN3_LNS$_{332\text{-}562}$, CLSTN3_2CAD$_{20\text{-}259}$, CLSTN3_2CAD_LNS$_{20\text{-}562}$ and CLSTN3_Full ectodomain$_{20\text{-}847}$ were 41, 40, 49 and 58, respectively

5. DISCUSSION

CLSTN3 together with NRXNs play a role in neuronal development by having an effect on synapse differentiation. The synaptic function of CLSNT3 is based on the interaction between CLSTN3 and NRXNs, which makes it important to understand, how the interaction is mediated between CLSTN3 and NRXNs. The previous studies about the interaction have had various results regarding the domains that are necessary for the interaction (Kim et al., 2020; Lu et al., 2014; Pettem et al., 2013; Um et al., 2014). Because of the disagreement over the interaction, the goal of this study was to purify the CLSTN3 ectodomain constructs, that could have been used to study the interaction between CLSTN3 and NRXNs, using pure proteins. Unfortunately, the attempt to purify the CAD domains of CLSTN3 failed and only the purification of the CLSTN3 LNS domain yielded enough pure protein to be used in a SEC-MALLS experiment from which the oligomerization of the LNS domain in a solution was determined.

The baculovirus were produced in the Sf9 cell cultures and the expression of the CLSTN3 ectodomain constructs was determined by western blotting. All of the baculovirus V_1 stocks mediated good expression of the protein constructs and the expression was at similar level among all of the constructs. However, the protein yields were small from all of the purification attempts when using the Sf9 cells. Therefore, the High Five cell cultures were decided to be used for the protein production. Comparison between the protein production in the High Five cell cultures and Sf9 cell cultures has revealed much higher protein yields from High Five cell cultures than Sf9 cell cultures. Then again, the virus particle production is significantly higher in the Sf9 cell cultures compared to the High Five cell cultures (Wilde et al., 2014). Thus, to get the optimal infection rate and protein yield from baculovirus expression system, it might be necessary to use Sf9 cell cultures for the virus particle production and High Five cell cultures for the protein production.

Even though there were several attempts, the purification of the CLSTN3 ectodomain constructs containing only the CAD domains or the construct containing the LNS and CAD domains was not successful. Because the expression and purification of the construct containing only the LNS domain yielded protein, it seemed that the problem in the purification was probably due to the CLSTN3 CAD domains. In the most recent study by Kim et al. (2020), the CLSTN3 constructs were successfully

produced and purified from HEK293T cell cultures. CLSTN3 ectodomain constructs can be produced in mammalian cell cultures, but the production in the insect cell cultures do not seem to produce stable-enough CLSTN3 constructs, containing the CAD domains, that could be purified. Thus, it is possible that the differences in the production of proteins between insect and mammalian cells is the reason why producing the construct, containing the CLSTN3 CAD domains, does not yield a stable-enough protein that could be purified. Perhaps, the next attempts of production and purification of the CLSTN3 CAD domains should be done using mammalian cell cultures, so that a stable protein could be produced, and it could be used in structural studies.

For the purified CLSTN3 LNS domain construct, SEC-MALLS experiment was performed. This experiment revealed that CLSTN3 LNS domain forms dimers in a solution. This is consistent with a previous study, that reported LNS domain dimerization for the human sex hormone-binding globulin LNS domain (Dales et al., 2000). However, previous results concerning the CLSTN3 oligomerization suggests that CLSTN3 forms monomers and tetramers and dimerization of CLSTN3 has not been observed (Lu et al., 2014). Of course, the CAD domains of CLSTN3 might also have an effect on the oligomerization of CLSTN3. Thus, further conclusions cannot be made from the dimerization of the CLSTN3 LNS domain, that was observed during this study.

The binding between CLSTN3 and NRXNs was tested in a cell surface binding assay. The results of the cell surface binding assay suggest that CLSTN3 CAD domains bind NRXN-α, but CLSTN3 does not bind NRXN-β. However, the results from the cell surface binding assay were to some extent contradicting. The highest signal intensity, indicating the binding between the NRXN-α and the different CLSTN3 constructs, was observed for the construct containing only the CLSTN3 CAD domains. The signal intensity for the binding between NRXN-α and the CLSTN3 construct, containing the LNS and CAD domains, was the second highest, but it was significantly lower than the signal intensity for the construct containing only the CLSTN3 CAD domains. The signal intensity for the binding between NRXN-α and the CLSTN3 full ectodomain construct was at the same level as the signal measured from the negative control. These results would suggest that CLSTN3 CAD domains bind NRXN-α, but the presence of the LNS domain and the rest of the CLSTN3 ectodomain could impair the binding. Nevertheless, the cause for the lower signal intensity might be for example lower expression of the protein construct on the surface of the HEK293T cells or cell detachment from the wells while performing the assay. Because the results from the cell surface binding assay were contradicting, more optimization of the assay is necessary before these results are verified.

Even though the results from the cell surface binding study between CLSTN3 and NRXN-α were contradicting, the result is rather consistent with the latest study on the subject. The latest study from Kim *et al*. (2020) claims that CLSTN3 binding to the NRXNs is mediated by the CAD domains of CLSTN3. However, Kim *et al*. were also able to detect binding between CLSTN3 and NRXN-β, which was not distinguished in this study. The cell surface binding assay, that was performed to test the binding against NRXN-β, had some differences compared to the assay performed to test the binding against NRXN-α. Because the NRXN-β construct included a GST tag and not an Fc tag, like the NRXN-α construct, both primary and secondary antibodies were necessary for the detection of the binding. This resulted in one more incubation step in the cell surface binding assay, which might have affected the reliability of the assay. Additionally, positive control for the NRXN-β binding was not available and the functionality of the assay could not be confirmed. On that account, based on this master's thesis study, conclusions about the interaction between CLSTN3 and NRXN-β should not be made.

The discrepancies about the interaction between CLSTN3 and NRXNs remain. In order to resolve the disagreement over the interaction, more studies have to be conducted. Resolving the structure of CLSTN3 could be the pivotal step in finding out what are the binding domains that mediate the interaction between CLSTN3 and NRXNs. Because the CLSTNs have a sequence identity of ~50% with each other, structural data from either CLSTN1 or CLSTN2 could also help to resolve the disagreement.

6. ACKNOWLEDGEMENTS

The work for this master's thesis was done in the Kajander lab at the Institute of Biotechnology in Helsinki under the supervision of Tommi Kajander, Ph.D., and Sudeep Karki M.Sc.

I wish to thank my supervisor Tommi for providing me the opportunity to work under his supervision during this master's thesis project. I would also like to express my gratitude to him for all of the guidance, comments and help he has given me. To my second supervisor Sudeep, I wish to express my most sincere appreciation for his tutelage and support during this project. Special thanks to the other members of the Kajander lab, Satoshi Fudo, Ph.D., and Violeta Manole, Ph.D., who both contributed to this work by giving me guidance in the lab.

REFERENCES

Alther, T.A., Domanitskaya, E., and Stoeckli, E.T. (2016). Calsyntenin 1-mediated trafficking of axon guidance receptors regulates the switch in axonal responsiveness at a choice point. Development *143,* 994.

Araki, Y., Tomita, S., Yamaguchi, H., Miyagi, N., Sumioka, A., Kirino, Y., and Suzuki, T. (2003). Novel Cadherin-related Membrane Proteins, Alcadeins, Enhance the X11-like Protein-mediated Stabilization of Amyloid beta -Protein Precursor Metabolism. J. Biol. Chem. *278,* 49448-49458.

Araki, Y., Miyagi, N., Kato, N., Yoshida, T., Wada, S., Nishimura, M., Komano, H., Yamamoto, T., De Strooper, B., Yamamoto, K., and Suzuki, T. (2004). Coordinated metabolism of Alcadein and amyloid beta-protein precursor regulates FE65-dependent gene transactivation. The Journal of Biological Chemistry *279,* 24343.

Araki, Y., Kawano, T., Taru, H., Saito, Y., Wada, S., Miyamoto, K., Kobayashi, H., Ishikawa, H., Ohsugi, Y., Yamamoto, T.*, et al.* (2007). The novel cargo Alcadein induces vesicle association of kinesin-1 motor components and activates axonal transport. Embo J. *26,* 1475-1486.

Bac-to-Bac® Baculovirus Expression System: Life Technologies Corporation. (2015). Bac-to-Bac® Baculovirus Expression System: User guide. Retrieved from http://tools.thermofisher.com/content/sfs/manuals/bactobac_man.pdf

Dai, J., Aoto, J., and Südhof, T.,C. (2019). Alternative Splicing of Presynaptic Neurexins Differentially Controls Postsynaptic NMDA and AMPA Receptor Responses. Neuron *102,* 993-1008.e5.

Dales, D., Muller, Y.A., Grishkovskaya, I., Avvakumov, G.V., Sklenar, G., and Hammond, G.L. (2000). Crystal structure of human sex hormone-binding globulin: steroid transport by a laminin G-like domain. Embo J. 19, 504-512.

De Ramon Francàs, G., Alther, T., and Stoeckli, E.T. (2017). Calsyntenins Are Expressed in a Dynamic and Partially Overlapping Manner during Neural Development. Frontiers in Neuroanatomy *11,*

Esch, F., Keim, P., Beattie, E., Blacher, R., Culwell, A., Oltersdorf, T., McClure, D., and Ward, P. (1990). Cleavage of amyloid beta peptide during constitutive processing of its precursor. Science *248,* 1122-1124.

Etherton, M.R., Blaiss, C.A., Powell, C.M., and Südhof, T.,C. (2009). Mouse neurexin-1alpha deletion causes correlated electrophysiological and behavioural changes consistent with cognitive impairments. Proc. Natl. Acad. Sci. U. S. A. *106,* 17998.

Froger, A., and Hall, J.E. (2007). Transformation of plasmid DNA into E. coli using the heat shock method. Journal of Visualized Experiments : JoVE; J Vis Exp 253.

Glenner, G.G., and Wong, C.W. (1984). Alzheimer's disease: Initial report of the purification and characterization of a novel cerebrovascular amyloid protein. Biochem. Biophys. Res. Commun. *120,* 885-890.

Haass, C., A, Y.H., M, G.S., D, B.T., and D, J.S. (1993). beta-Amyloid peptide and a 3-kDa fragment are derived by distinct cellular mechanisms. J. Biol. Chem. *268,* 3021.

Hata, S., Fujishige, S., Araki, Y., Kato, N., Araseki, M., Nishimura, M., Hartmann, D., Saftig, P., Fahrenholz, F., Taniguchi, M.*, et al.* (2009). Alcadein Cleavages by Amyloid β-Precursor Protein (APP) α- and γ-Secretases Generate Small Peptides, p3-Alcs, Indicating Alzheimer Disease-related γ-Secretase Dysfunction. J. Biol. Chem. *284,* 36024-36033.

Hintsch, G., Zurlinden, A., Meskenaite, V., Steuble, M., Fink-Widmer, K., and Kinter, J. (2002). The Calsyntenins—A Family of Postsynaptic Membrane Proteins with Distinct Neuronal Expression Patterns. Molecular and Cellular Neuroscience *21,* 393-409.

Hoerndli, F.J., Walser, M., Fröhli Hoier, E., de Quervain, D., Papassotiropoulos, A., and Hajnal, A. (2009). A conserved function of c. elegans CASY-1 calsyntenin in associative learning. PloS one 4.3 e4880–e4880. Web.

Ichtchenko, K., Hata, Y., Nguyen, T., Ullrich, B., Missler, M., Moomaw, C., and Südhof, T.,C. (1995). Neuroligin 1: A splice site-specific ligand for β-neurexins. Cell *81,* 435-443.

Ikeda, D.D., Duan, Y., Matsuki, M., Kunitomo, H., Hutter, H., Hedgecock, E.M., and Iino, Y. (2008). CASY-1, an ortholog of calsyntenins/alcadeins, is essential for learning in Caenorhabditis elegans. Proceedings of the National Academy of Sciences of the United States *105,* 5260.

Jacobsen, L.K., Picciotto, M.R., Heath, C.J., Mencl, W.E., and Gelernter, J. (2009). Allelic Variation of Calsyntenin 2 (CLSTN2) Modulates the Impact of Developmental Tobacco Smoke Exposure on Mnemonic Processing in Adolescents. Biol. Psychiatry *65,* 671-679.

Jarrett, J.T., Berger, E.P., and Lansbury, P.T. (1993). The carboxy terminus of the .beta. amyloid protein is critical for the seeding of amyloid formation: Implications for the pathogenesis of Alzheimer's disease. Biochemistry *32,* 4693-4697.

Kattenstroth, G., Tantalaki, E., Südhof, T.C., Gottmann, K., and Missler, M. (2004). Postsynaptic N-Methyl-D-Aspartate Receptor Function Requires α-Neurexins. Proc. Natl. Acad. Sci. U. S. A. *101,* 2607-2612.

Keinänen, K., Jouppila, A., and Kuusinen, A. (1998). Characterization of the kainate-binding domain of the glutamate receptor GluR-6 subunit. Biochem. J. *330,* 1461-1467.

Kim, H., Kim, D., Kim, J., Lee, H., Park, D., Kang, H., Matsuda, K., Sterky, F.H., Yuzaki, M., Kim, J.Y., Choi, S., Ko, J., and Um, J.W. (2020). Calsyntenin-3 interacts with both α- and β-neurexins in the regulation of excitatory synaptic innervation in specific Schaffer collateral pathways. J. Biol. Chem. *295,* 9244-9262.

Ko, J., Fuccillo, M.V., Malenka, R.C., and Südhof, T.,C. (2009). LRRTM2 Functions as a Neurexin Ligand in Promoting Excitatory Synapse Formation. Neuron *64,* 791-798.

Konecna, A., Frischknecht, R., Kinter, J., Ludwig, A., Steuble, M., Meskenaite, V., Indermühle, M., Engel, M., Cen, C., Mateos, J., Streit, P., and Sonderegger, P. (2006). Calsyntenin-1 docks vesicular cargo to kinesin-1. Mol. Biol. Cell *17,* 3651.

Laukka, E.J., Lövdén, M., Herlitz, A., Karlsson, S., Ferencz, B., Pantzar, A., Keller, L., Graff, C., Fratiglioni, L., and Bäckman, L. (2013). Genetic Effects on Old-Age Cognitive Functioning: A Population-Based Study. Psychol. Aging *28,* 262-274.

Lee, T.J., Lee, J.W., Haynes, E.M., Eliceiri, K.W., and Halloran, M.C. (2017). The Kinesin Adaptor Calsyntenin-1 Organizes Microtubule Polarity and Regulates Dynamics during Sensory Axon Arbor Development. Frontiers in Cellular Neuroscience *11,* 107.

Lipina, T.V., Prasad, T., Yokomaku, D., Luo, L., Connor, S.A., Kawabe, H., Wang, Y.T., Brose, N., Roder, J.C., and Craig, A.M. (2016). Cognitive Deficits in Calsyntenin-2-deficient Mice Associated with Reduced GABAergic Transmission. Neuropsychopharmacology : Official Publication of the American College of Neuropsychopharmacology *41,* 802.

Ludwig, A., Blume, J., Diep, T., Yuan, J., Mateos, J.M., Leuthäuser, K., Steuble, M., Streit, P., and Sonderegger, P. (2009). Calsyntenins Mediate TGN Exit of APP in a Kinesin-1-Dependent Manner. Traffic *10,* 572-589.

Manchester, K.L. (1996). Use of UV Methods for Measurement of Protein and Nucleic Acid Concentrations. BioTechniques *20,* 968-970.

Maruta, C., Saito, Y., Hata, S., Gotoh, N., Suzuki, T., and Yamamoto, T. (2012). Constitutive Cleavage of the Single-Pass Transmembrane Protein Alcadeinα Prevents Aberrant Peripheral Retention of Kinesin-1 (Alcadein Cleavage for Kinesin-1 Distribution).

Missler, M., Zhang, W., Rohlmann, A., Kattenstroth, G., Hammer, R.E., Gottmann, K., and Südhof, T.,C. (2003). α-Neurexins couple Ca2+ channels to synaptic vesicle exocytosis. Nature *423,* 939-948.

Pantzar, A., Laukka, E.J., Atti, A.R., Papenberg, G., Keller, L., Graff, C., Fratiglioni, L., and Bäckman, L. (2014). Interactive effects of KIBRA and CLSTN2 polymorphisms on episodic memory in old-age unipolar depression. Neuropsychologia *62,* 137-142.

Papassotiropoulos, A., Stephan, D., Huentelman, M., and Hoerndli, F. (2006). Common Kibra Alleles Are Associated with Human Memory Performance. Science (Wash.) *314,* 474-478.

Pettem, K.l., Yokomaku, D., Luo, L., Linhoff, M.w., Prasad, T., Connor, S.a., Siddiqui, T.j., Kawabe, H., Chen, F., Zhang, L*., et al.* (2013). The Specific α-Neurexin Interactor Calsyntenin-3 Promotes Excitatory and Inhibitory Synapse Development. Neuron *80,* 113-128.

Ponomareva, O.Y., Holmen, I.C., Sperry, A.J., Eliceiri, K.W., and Halloran, M.C. (2014). Calsyntenin-1 regulates axon branching and endosomal trafficking during sensory neuron development in vivo. The Journal of Neuroscience : The Official Journal of the Society for Neuroscience *34,* 9235.

Preuschhof, C., Heekeren, H.R., Li, S., Sander, T., Lindenberger, U., and Bäckman, L. (2010). KIBRA and CLSTN2 polymorphisms exert interactive effects on human episodic memory. Neuropsychologia *48,* 402-408.

Reichelt, A.C., Rodgers, R.J., and Clapcote, S.J. (2012). The role of neurexins in schizophrenia and autistic spectrum disorder. Neuropharmacology *62,* 1519-1526.

Seubert, P., Oltersdorf, T., Lee, M.G., Barbour, R., Blomquist, C., Davis, D.L., Bryant, K., Fritz, L.C., Galasko, D., Thal, L.J., Lieberburg, I., and Schenk, D.B. (1993). Secretion of β-amyloid precursor protein cleaved at the amino terminus of the β-amyloid peptide. Nature *361,* 260-263.

Shi, X., and Jarvis, D.L. (2007). Protein N-glycosylation in the baculovirus-insect cell system. Curr. Drug Targets *8,* 1116-1125.

Siddiqui, T.J., Pancaroglu, R., Kang, Y., Rooyakkers, A., and Craig, A.M. (2010). LRRTMs and neuroligins bind neurexins with a differential code to cooperate in glutamate synapse development. J. Neurosci. *30,* 7495-7506.

Siddiqui, T., Tari, P.K., Connor, S.A., Zhang, P., Dobie, F.A., She, K., Kawabe, H., Wang, Y., Brose, N., and Craig, A. (2013). An LRRTM4-HSPG Complex Mediates Excitatory Synapse Development on Dentate Gyrus Granule Cells. Neuron *79,* 680-695.

Sievers, F., Wilm, A., Dineen, D., Gibson, T.J., Karplus, K., Li, W., Lopez, R., Mcwilliam, H., Remmert, M., Söding, J., Thompson, J.D., and Higgins, D.G. (2011). Fast, scalable generation of high-quality protein multiple sequence alignments using Clustal Omega. Molecular Systems Biology *7,* n/a.

Sons, M.S., Busche, N., Strenzke, N., Moser, T., Ernsberger, U., Mooren, F.C., Zhang, W., Ahmad, M., Steffens, H., Schomburg, E.D., Plomp, J.J., and Missler, M. (2006). α-Neurexins are required for efficient transmitter release and synaptic homeostasis at the mouse neuromuscular junction. Neuroscience *138,* 433-446.

Ster, J., Steuble, M., Orlando, C., Diep, T., Akhmedov, A., Raineteau, O., Pernet, V., Sonderegger, P., and Gerber, U. (2014). Calsyntenin-1 regulates targeting of dendritic NMDA receptors and dendritic spine maturation in CA1 hippocampal pyramidal cells during postnatal development. The Journal of Neuroscience : The Official Journal of the Society for Neuroscience *34,* 8716.

Steuble, M., Diep, T.M., Schatzle, P., Ludwig, A., Tagaya, M., Kunz, B., and Sonderegger, P. (2012). Calsyntenin-1 shelters APP from proteolytic processing during anterograde axonal transport. Biology Open *1,* 761-774.

Steuble, M., Gerrits, B., Ludwig, A., Mateos, J.M., Diep, T., Tagaya, M., Stephan, A., Schätzle, P., Kunz, B., Streit, P., and Sonderegger, P. (2010). Molecular characterization of a trafficking organelle: Dissecting the axonal paths of calsyntenin-1 transport vesicles. Proteomics *10,* 3775-3788.

Thapliyal, S., Vasudevan, A., Dong, Y., Bai, J., Koushika, S.P., and Babu, K. (2018). The C-terminal of CASY-1/Calsyntenin regulates GABAergic synaptic transmission at the Caenorhabditis elegans neuromuscular junction. PLoS Genetics *14,* e1007263.

Ullrich, B., Ushkaryov, Y.A., and Südhof, T.,C. (1995). Cartography of neurexins: More than 1000 isoforms generated by alternative splicing and expressed in distinct subsets of neurons. Neuron *14,* 497-507.

Um, J., Pramanik, G., Ko, J.s., Song, M., Lee, D., Kim, H., Park, K., Südhof, T.c., Tabuchi, K., and Ko, J. (2014). Calsyntenins Function as Synaptogenic Adhesion Molecules in Concert with Neurexins. Cell Reports *6,* 1096-1109.

Ushkaryov, Y.A., Hata, Y., Ichtchenko, K., Moomaw, C., Afendis, S., Slaughter, C.A., and Südhof, T.C. (1994). Conserved domain structure of beta-neurexins. Unusual cleaved signal sequences in receptor-like neuronal cell-surface proteins. The Journal of Biological Chemistry *269,* 11987.

Ushkaryov, Y., Petrenko, A., Geppert, M., and Südhof, T. (1992). Neurexins: Synaptic cell surface proteins related to the alpha -latrotoxin receptor and laminin. Science (Wash.) *257,* 50-56.

Ushkaryov, Y., and Südhof, T. (1993). Neurexin III(alpha): Extensive alternative splicing generates membrane-bound and soluble forms. Proc. Natl. Acad. Sci. U. S. A. *90,* 6410.

Vogt, L., Schrimpf, S.P., Meskenaite, V., Frischknecht, R., Kinter, J., Leone, D.P., Ziegler, U., and Sonderegger, P. (2001). Calsyntenin-1, a Proteolytically Processed Postsynaptic Membrane Protein with a Cytoplasmic Calcium-Binding Domain. Molecular and Cellular Neuroscience *17,* 151-166.

Wang, G., de Jong, R.,N., van den Bremer, Ewald T.,J., Parren, Paul W. H. I., and Heck, A.J.R. (2017). Enhancing Accuracy in Molecular Weight Determination of Highly Heterogeneously Glycosylated Proteins by Native Tandem Mass Spectrometry. Anal. Chem. (Wash.) *89,* 4793-4797.

Wilde, M., Klausberger, M., Palmberger, D., Ernst, W., and Grabherr, R. (2014). Tnao38, high five and Sf9—evaluation of host–virus interactions in three different insect cell lines: baculovirus production and recombinant protein expression. Biotechnol. Lett. *36,* 743-749.

Zhang, C., Atasoy, D., Araç, D., Yang, X., Fucillo, M.V., Robison, A.J., Ko, J., Brunger, A.T., and Südhof, T.,C. (2010a). Neurexins Physically and Functionally Interact with GABA A Receptors. Neuron *66,* 403-416.

Zhang, C., Atasoy, D., Araç, D., Yang, X., Fucillo, M.V., Robison, A.J., Ko, J., Brunger, A.T., and Südhof, T.,C. (2010b). Neurexins Physically and Functionally Interact with GABA A Receptors. Neuron *66,* 403-416.

Zhang, W., Rohlmann, A., Sargsyan, V., Aramuni, G., Hammer, R.E., Südhof, T.,C., and Missler, M. (2005). Extracellular domains of alpha-neurexins participate in regulating synaptic transmission by selectively affecting N- and P/Q-type Ca2+ channels. J. Neurosci. *25,* 4330-4342.

APPENDICES

APPENDIX 1

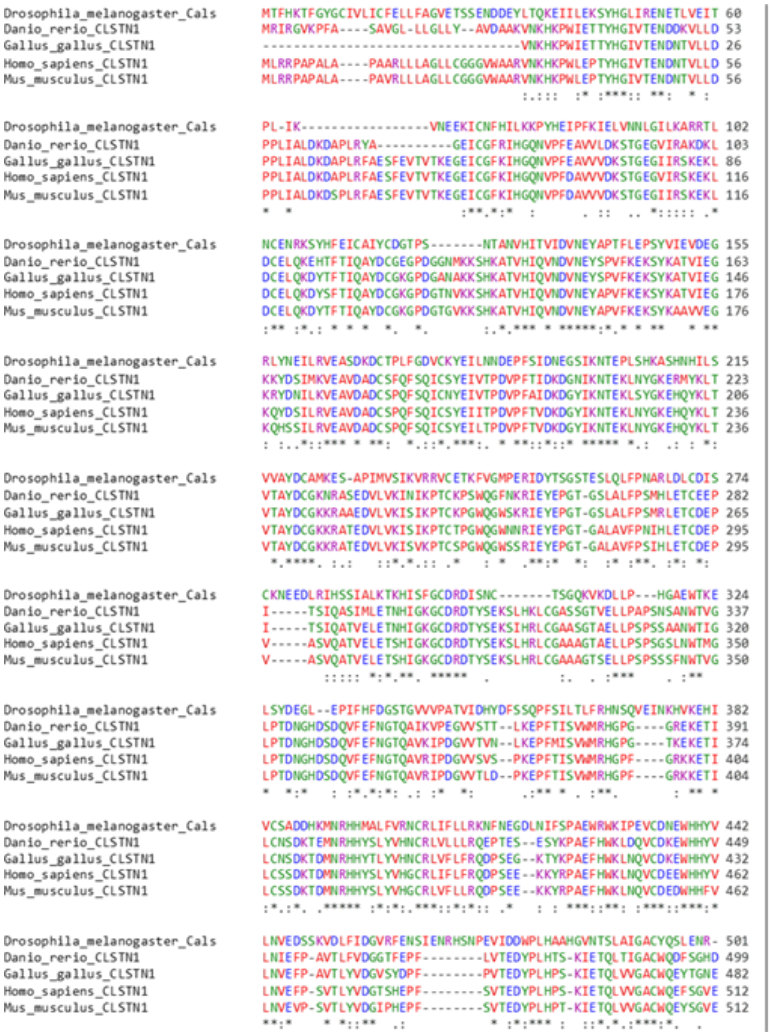

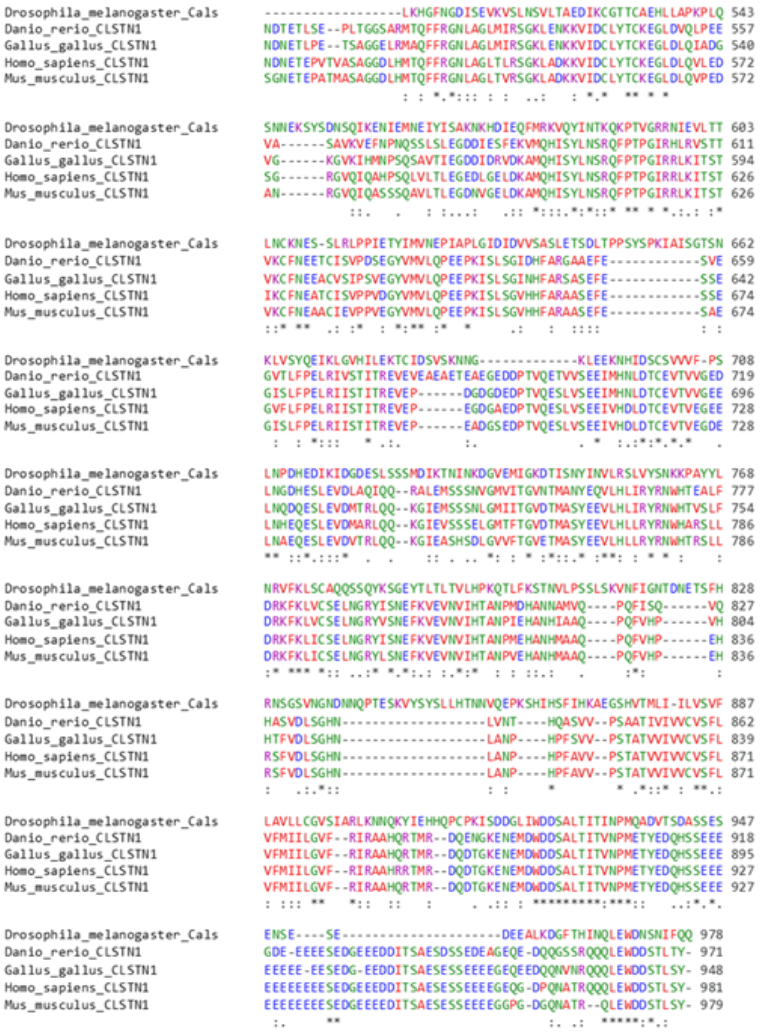

Appendix 1.1 Calsyntenin-1 Sequence Alignment

Sequence alignment of *D. melanogaster* Cals and human, mouse, chicken and zebrafish calsyntenin-1 gene sequences.

Appendix 1.2 Sequence Percent Identity Matrix of Calsyntenin-1 Genes

	Drosophila melanogaster	***Danio rerio***	***Gallus gallus***	***Homo sapiens***	***Mus musculus***
Drosophila melanogaster	100	31.97	33.49	32.84	33.03
Danio rerio	31.97	100	81.09	76.48	74.66
Gallus gallus	33.49	81.09	100	86.27	84.76
Homo sapiens	32.84	76.48	86.27	100	92.65
Mus musculus	33.03	74.66	84.76	92.65	100

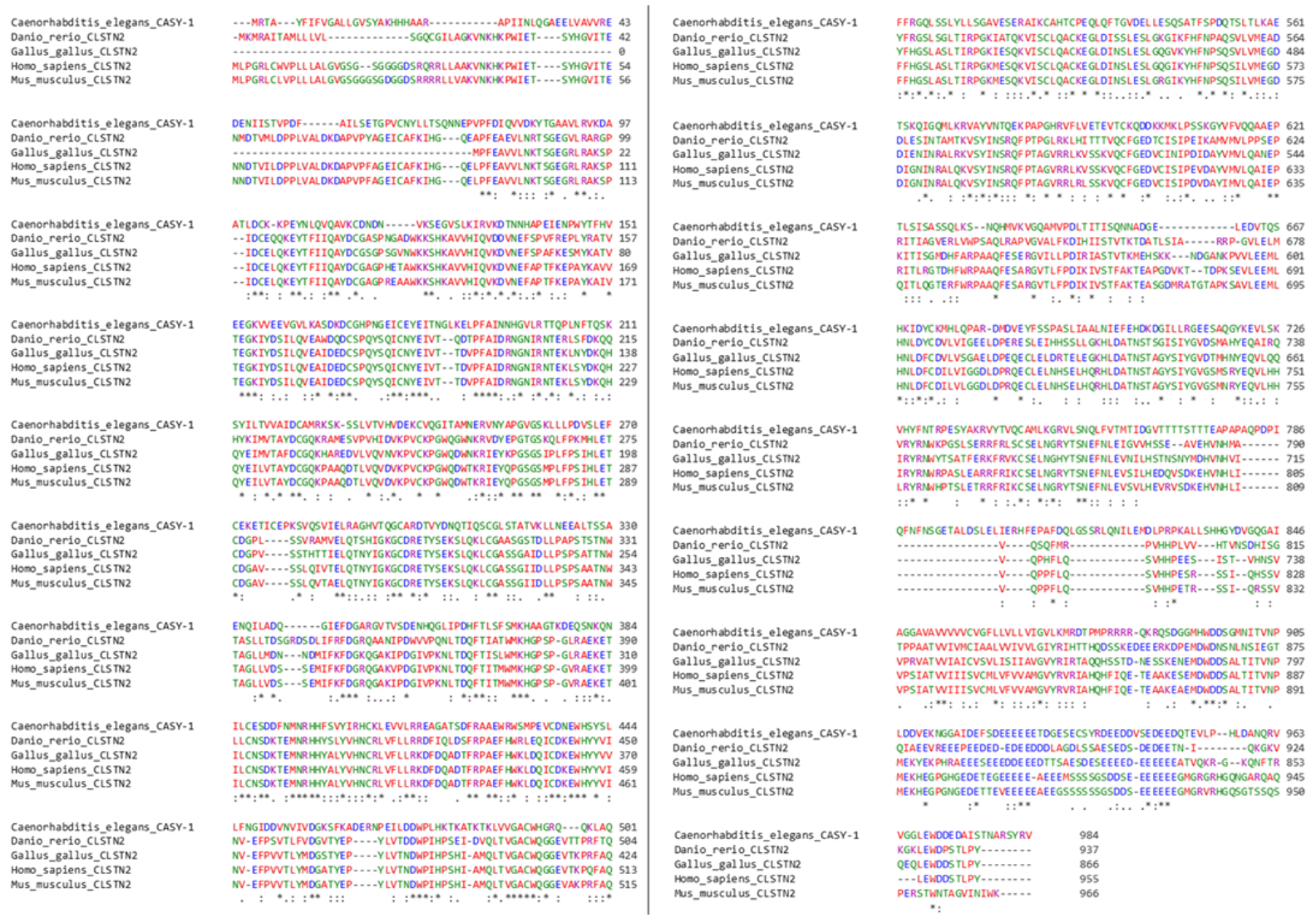

Appendix 1.3 Calsyntenin-2 Sequence Alignment

Sequence alignment of *C. elegans* CASY-1 and human, mouse, chicken and zebrafish calsyntenin-2 gene sequences.

Appendix 1.4 Sequence Percent Identity Matrix of Calsyntenin-2 Genes

	Caenorhabditis elegans	*Danio rerio*	*Gallus gallus*	*Homo sapiens*	*Mus musculus*
Caenorhabditis elegans	100	28.94	29.88	28.98	27.71
Danio rerio	28.94	100	66.78	66.88	65.74
Gallus gallus	29.88	66.78	100	79.65	77.83
Homo sapiens	28.98	66.88	79.65	100	92.98
Mus musculus	27.71	65.74	77.83	92.98	100

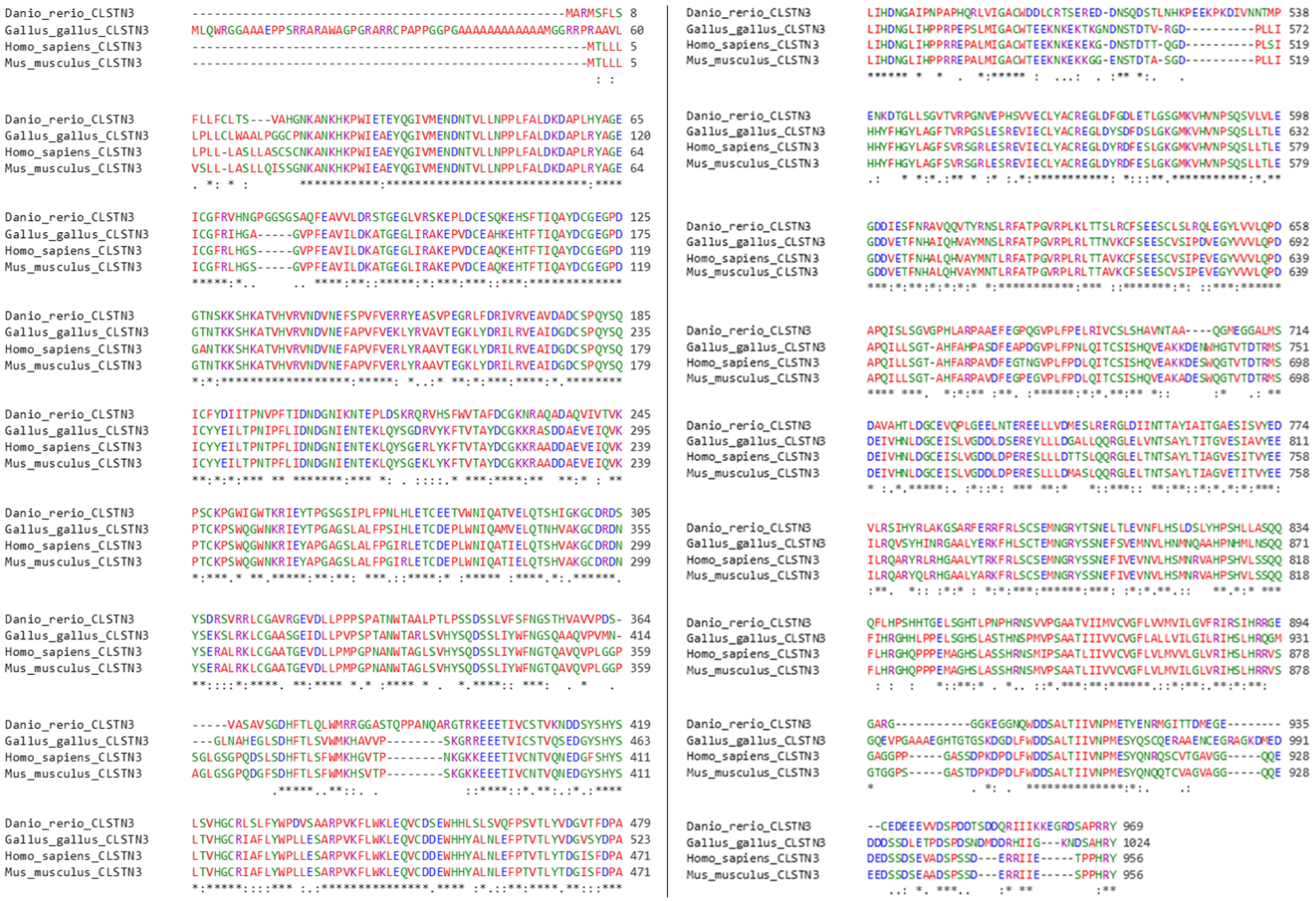

Appendix 1.5 Calsyntenin-3 Sequence Alignment

Sequence alignment human, mouse, chicken and zebrafish calsyntenin-3 gene sequences.

Appendix 1.6 Sequence Percent Identity Matrix of Calsyntenin-2 Genes

	Danio rerio	*Gallus gallus*	*Homo sapiens*	*Mus musculus*
Danio rerio	100	59.94	61.80	61.70
Gallus gallus	59.94	100	82.77	82.98
Homo sapiens	61.80	82.77	100	95.71
Mus musculus	61.70	82.98	95.71	100

The alignments and the percent identity matrices were created using Clustal Omega, multiple sequence alignment tool (Sievers et al., 2011).

APPENDIX 2

Appendix 2.1 Primers Used in the Cloning of CLSTN3 Ectodomain Constructs

Construct	Forward Primer	Reverse Primer
CLSTN3_2CAD_LNS$_{6His_20-562}$	CLSTN3_6His3_F	CLSTN3_332_562_R
CLSTN3_2CAD_LNS$_{36-562}$	CLSTN36_3_F	CLSTN3_332_562_R
CLSTN3_2CAD$_{6His_20-259}$	CLSTN3_6His3_F	CLSTN3_20_259_R
CLSTN3_2CAD$_{6His_36-259}$	CLSTN36_6His3_F	CLSTN3_20_259_R
CLSTN3_LNS6His_332-562_Fc	CLSTN3_332_548_F	CLSTN3_332_562_R

Appendix 2.2 Primer Sequences

Primer name	Sequence
CLSTN3_6His3_F	atatatGAATTCCATCATCATCATCATCATaacaaagccaacaagcacaag
CLSTN36_3_F	atatatGAATTCATCGAGGCAGAGTACCAGG
CLSTN36_6His3_F	atatatGAATTCCATCATCATCATCATCATATCGAGGCAGAGTACCAGG
CLSTN3_332_548_F	atatatGAATTCTCGGTGCACTACAGCCAG
CLSTN3_332_562_R	ATATATGGATCCGCCCAGGCTCTCGAAATC
CLSTN3_20_259_R	ATATATGGATCCggctcctggggcatattc

APPENDIX 3

Appendix 3 The Protein Yields from the Sf9 Cell Cultures

Construct	Infection ratio	Protein yield
CLSTN3_2CAD_LNS$_{6His_20-562}$	1:1000	0.29 mg
	1:200	0.90 mg
CLSTN3_2CAD_LNS$_{36-562}$	1:1000	0.74 mg
	1:200	0.64 mg
CLSTN3_2CAD$_{6His_36-259}$	1:1000	0.72 mg
	1:200	1.18 mg
CLSTN3_LNS6His_332-562_Fc	1:1000	1.0 mg
	1:200	0.93 mg

APPENDIX 4

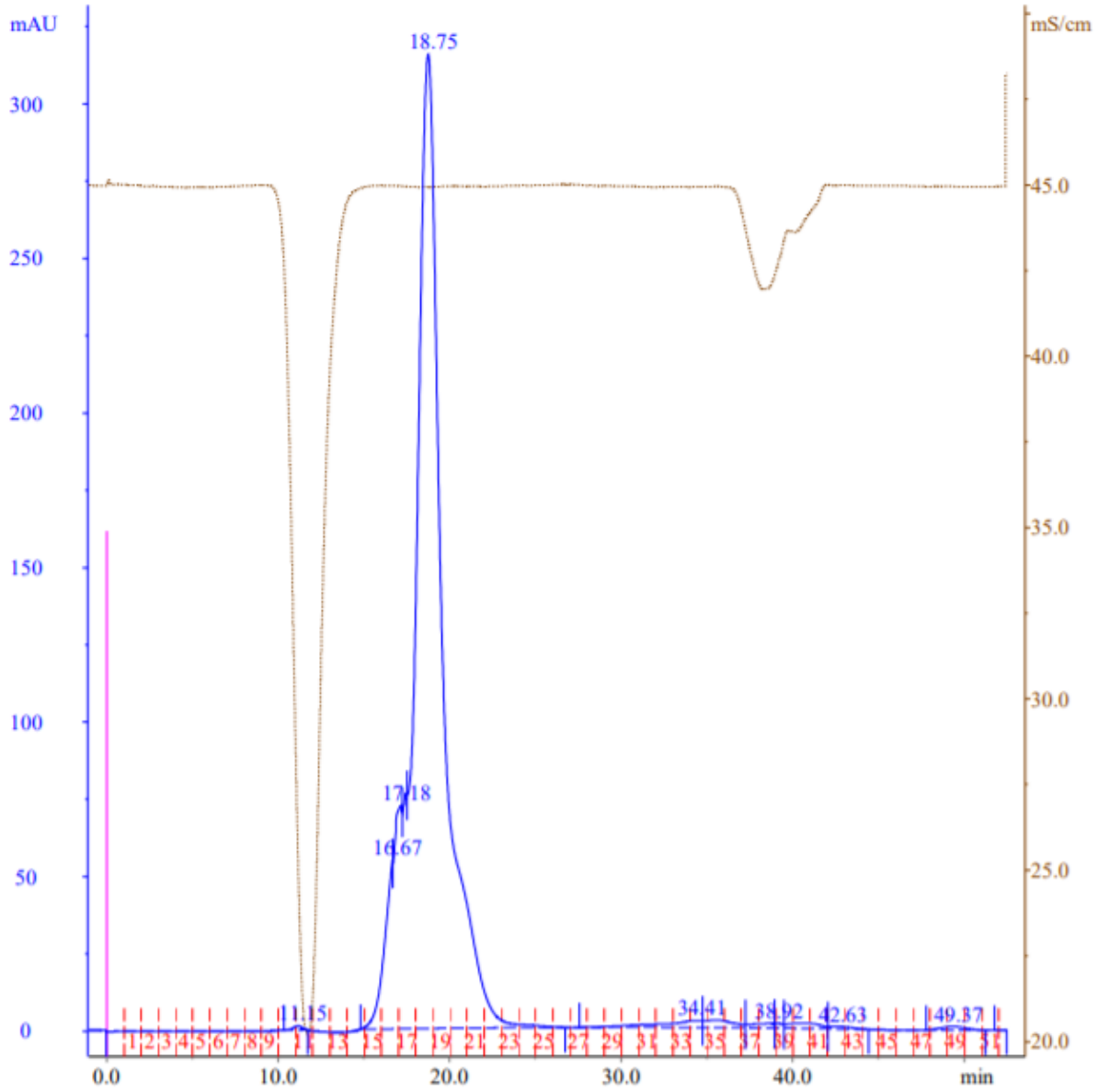

Appendix 4 Gel Filtration Profile from the Size-exclusion Chromatography of the CLSTN3_LNS6His_332-562_Fc Ectodomain Construct